

CONSTRUCTION AND EVALUATION OF PH CURVES IN EXPONENTIAL-POLYNOMIAL SPACES *

LUCIA ROMANI AND ALBERTO VISCARDI[†]

Abstract. In the past few decades polynomial curves with Pythagorean Hodograph (for short PH curves) have received considerable attention due to their usefulness in various CAD/CAM areas, manufacturing, numerical control machining and robotics. This work deals with classes of PH curves built-upon exponential-polynomial spaces (for short EPH curves). In particular, for the two most frequently encountered exponential-polynomial spaces, we first provide necessary and sufficient conditions to be satisfied by the control polygon of the Bézier-like curve in order to fulfill the PH property. Then, for such EPH curves, fundamental characteristics like parametric speed or cumulative and total arc length are discussed to show the interesting analogies with their well-known polynomial counterparts. Differences and advantages with respect to ordinary PH curves become commendable when discussing the solutions to application problems like the interpolation of first-order Hermite data. Finally, a new evaluation algorithm for EPH curves is proposed and shown to compare favorably with the celebrated de Casteljau-like algorithm and two recently proposed methods: Woźny and Chudy’s algorithm and the dynamic evaluation procedure by Yang and Hong.

Key words. exponential-polynomial curves, B-basis, evaluation, stability, pythagorean hodograph

AMS subject classifications. 65D17, 65D18, 65Y20

1. Introduction. Ordinary polynomial curve segments with the Pythagorean-Hodograph (PH) property have been extensively studied [3], and their construction has been satisfactorily extended also to spaces spanned by algebraic-trigonometric polynomials [2, 5, 6, 10, 11]. Although spaces spanned by algebraic-hyperbolic polynomials have close analogies with the ones spanned by algebraic-trigonometric polynomials (see section 2), on the one hand they offer unexpected advantages and, on the other hand, their handling might require some additional caution which is important to underline. Indeed, in the remainder of this manuscript we first show (see sections 3 and 4) that the constraints to be satisfied by the control points of the algebraic-hyperbolic Bézier curve segments in order to achieve the PH property, mimic very closely the necessary and sufficient conditions known in the polynomial and algebraic-trigonometric cases. In addition, also the computed expressions for their fundamental characteristics (parametric speed or cumulative and total arc length) sound to be very similar. But, when used in application contexts like solving first-order Hermite interpolation problems (see section 5), algebraic-hyperbolic Bézier curves offer the crucial advantage of being always able to provide regular curves without undesired loops or self-intersections. For instance, when considering the planar Hermite data of Figure 1, none of the solutions provided by the ordinary polynomial PH quintics are free of loops. Instead, when the same Hermite problem is solved by using algebraic-trigonometric PH (for short ATPH) curves, for a suitable choice of the free parameter one good solution exists (see Figure 1 bottom). The further advantage offered by EPH curves (or algebraic-hyperbolic PH curves) is clearly shown in Figure 2: depending on the selected value of the exponential shape parameter ω we can obtain different good solutions and, for small values of ω , we can also recover the shape of the solution

*

Funding: This work was partially funded by INdAM-GNCS 2020 project “Interpolation and smoothing: theoretical, computational and applied aspects” (Prot. U-UFMBAZ-2020-000564).

[†]AM² - Dipartimento di Matematica, Alma Mater Studiorum Università di Bologna, Bologna, Italy (lucia.romani@unibo.it, alberto.viscardi@unibo.it).

provided by the ATPH. In other words, even if ATPH curves are also equipped with a shape parameter α (see [10, 11]), they can achieve a more limited number of shapes than algebraic-hyperbolic PH (hereafter also called EPH) curves. This is of course a practical reason that motivates the study of EPH curves. An additional reason that prompted us to investigate algebraic-hyperbolic PH curves arises from the observation that, even if the hyperbolic cosine and sine are just the opposite side of the exponential coin from the trigonometric cosine and sine, the normalized B-basis (also known as Chebyshevian Bernstein basis) of the underlying Extended Chebyshev (EC) space is known to be affected by numerical instability when large exponential shape parameters are selected [12]. Thus, one of the main goals of this work is also to suggest a stable formulation of the normalized B-basis of the two exponential-polynomial spaces (or, more precisely, algebraic-hyperbolic spaces) that are most frequently encountered when working with non-polynomial PH curves, so that numerical instabilities are avoided. Furthermore, for such spaces, we aim at proposing a novel evaluation algorithm that is stable for a wide range of the exponential shape parameter, in contrast to the dynamic evaluation procedure in [15], and has a lower computational time (see section 6), compared with the de Casteljau-like B-algorithm [1, 7, 8, 9] (analogue of the de Casteljau algorithm for classical polynomial Bézier curves), and with the algorithm introduced by Woźny and Chudy in [13].

2. PH curves in exponential-polynomial spaces: EPH curves. Let $m \in \mathbb{N}_0$ and $\omega \in \mathbb{R}^+$, where $\mathbb{N}_0 = \mathbb{N} \cup \{0\}$ and \mathbb{R}^+ denotes the set of positive real numbers.

DEFINITION 2.1 (Exponential-polynomial spaces). *We define, in terms of m and ω , the following spaces of exponential polynomials*

$$\mathcal{EP}_m^\omega := \text{span} \left\{ \{1, t\} \cup \bigcup_{k=1}^m \{e^{k\omega t}, e^{-k\omega t}\} \right\},$$

and

$$\mathcal{OEP}_m^\omega := \text{span} \left\{ \{1, t\} \cup \bigcup_{k=1}^m \{e^{(2k-1)\omega t}, e^{-(2k-1)\omega t}\} \right\}.$$

We observe that

$$\mathcal{OEP}_0^\omega = \mathcal{EP}_0^\omega = \text{span} \{1, t\}, \quad \mathcal{OEP}_1^\omega = \mathcal{EP}_1^\omega = \text{span} \{1, t, e^{\omega t}, e^{-\omega t}\},$$

but, for $m > 1$, $\mathcal{OEP}_m^\omega \subsetneq \mathcal{EP}_{2m-1}^\omega$. Moreover, denoting with \mathcal{D} the differential operator d/dt , it is easy to check that

$$\mathcal{DEP}_m^\omega = \text{span} \left\{ \{1\} \cup \bigcup_{k=1}^m \{e^{k\omega t}, e^{-k\omega t}\} \right\} \subset \mathcal{EP}_m^\omega,$$

$$\mathcal{D}^2 \mathcal{EP}_m^\omega = \text{span} \left\{ \bigcup_{k=1}^m \{e^{k\omega t}, e^{-k\omega t}\} \right\} \subset \mathcal{DEP}_m^\omega,$$

and similarly

$$\mathcal{DOEP}_m^\omega = \text{span} \left\{ \{1\} \cup \bigcup_{k=1}^m \{e^{(2k-1)\omega t}, e^{-(2k-1)\omega t}\} \right\} \subset \mathcal{OEP}_m^\omega,$$

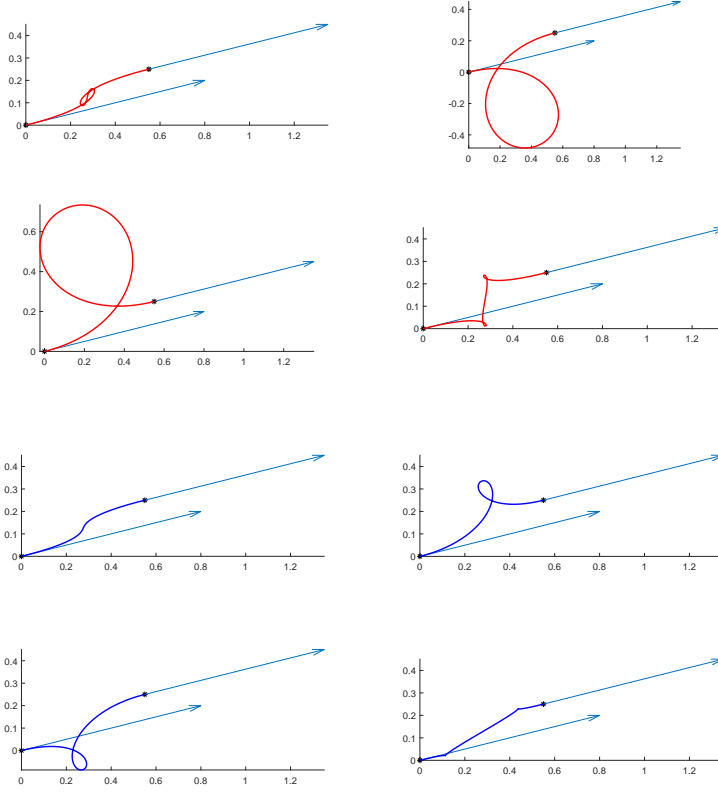


FIG. 1. Top: The four planar PH interpolants to the points $\mathbf{r}_0 = (0,0)$, $\mathbf{r}_5 = (0.55,0.25)$ and associated first derivatives $\mathbf{d}_i = (4,1)$, $\mathbf{d}_f = (4,1)$ (here plotted with a scale factor of $1/5$ to fit into the picture). Bottom: The four planar ATPH interpolants to the same Hermite data, obtained with the shape parameter $\alpha = \pi/6$ (see [11]).

$$\mathcal{D}^2\mathcal{OEP}_m^\omega = \text{span} \left\{ \bigcup_{k=1}^m \{e^{(2k-1)\omega t}, e^{-(2k-1)\omega t}\} \right\} \subset \mathcal{DOEP}_m^\omega.$$

Again, we observe that

$$\mathcal{DOEP}_0^\omega = \mathcal{DEP}_0^\omega = \text{span} \{1\}, \quad \mathcal{DOEP}_1^\omega = \mathcal{DEP}_1^\omega = \text{span} \{1, e^{\omega t}, e^{-\omega t}\},$$

$$\mathcal{D}^2\mathcal{OEP}_0^\omega = \mathcal{D}^2\mathcal{EP}_0^\omega = \{0\}, \quad \mathcal{D}^2\mathcal{OEP}_1^\omega = \mathcal{D}^2\mathcal{EP}_1^\omega = \text{span} \{e^{\omega t}, e^{-\omega t}\},$$

but, for $m > 1$, $\mathcal{DOEP}_m^\omega \subsetneq \mathcal{DEP}_{2m-1}^\omega$ and $\mathcal{D}^2\mathcal{OEP}_m^\omega \subsetneq \mathcal{D}^2\mathcal{EP}_{2m-1}^\omega$.

DEFINITION 2.2 (PH curve in \mathcal{EP}_m^ω). A parametric curve $\mathbf{r} : [0, 1] \rightarrow \mathbb{R}^d$, $d \in \{2, 3\}$, is called a PH curve in \mathcal{EP}_m^ω if and only if one of the following holds

- (planar EPH curve) $d = 2$, $\mathbf{r}(t) = (x(t), y(t))$, $x, y \in \mathcal{EP}_m^\omega$, with

$$(2.1) \quad \begin{cases} x'(t) = a_1(t)^2 - a_2(t)^2, \\ y'(t) = 2a_1(t)a_2(t), \end{cases}$$

for some exponential polynomials a_1, a_2 .

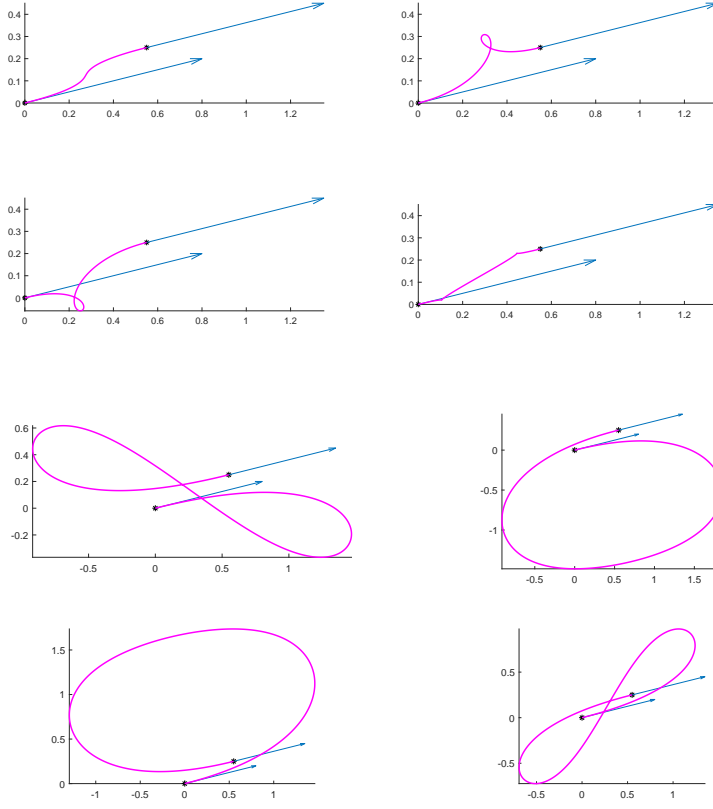


FIG. 2. Planar EPH interpolants to the points $\mathbf{r}_0 = (0, 0)$, $\mathbf{r}_5 = (0.55, 0.25)$ and associated first derivatives $\mathbf{d}_i = (4, 1)$, $\mathbf{d}_f = (4, 1)$ (here plotted with a scale factor of 1/5 to fit into the picture). Top: the four solutions obtained with the exponential shape parameter $\omega = 0.5$. Bottom: the four solutions obtained with the exponential shape parameter $\omega = 8$.

- (spatial EPH curve) $d = 3$, $\mathbf{r}(t) = (x(t), y(t), z(t))$, $x, y, z \in \mathcal{EP}_m^\omega$, with

$$(2.2) \quad \begin{cases} x'(t) = a_0(t)^2 + a_1(t)^2 - a_2(t)^2 - a_3(t)^2, \\ y'(t) = 2(a_1(t)a_2(t) + a_0(t)a_3(t)), \\ z'(t) = 2(a_1(t)a_3(t) - a_0(t)a_2(t)), \end{cases}$$

for some exponential polynomials a_0, a_1, a_2, a_3 .

Remark 2.3. The curves defined via (2.1) and (2.2) are regular if and only if the exponential polynomials a_k do not have a common root in $[0, 1]$ (see, e.g., [3]).

In what follows we only consider the case $d = 3$, i.e., spatial curves: planar curves ($d = 2$) can be easily obtained setting $a_0(t) = a_3(t) = 0$ since this condition and (2.2) imply (2.1) along with $z(t) = 0$. From (2.2) then, it is easy to get

$$x'(t)^2 + y'(t)^2 + z'(t)^2 = (a_0(t)^2 + a_1(t)^2 + a_2(t)^2 + a_3(t)^2)^2.$$

Thus, the defining characteristic of a PH curve in \mathcal{EP}_m^ω is the fact that the coordinate components of its derivative (or hodograph) comprise a Pythagorean d -tuple of functions in \mathcal{DEP}_m^ω - i.e., the sum of their squares coincides with the perfect square

of a function in \mathcal{DEP}_m^ω . By virtue of this remarkable property, the parametric speed of the curve $\sigma(t) = |\mathbf{r}'(t)|$ satisfies

$$\sigma(t) = a_0(t)^2 + a_1(t)^2 + a_2(t)^2 + a_3(t)^2.$$

Clearly, a plethora of combinations of exponential polynomials a_k exists so that (2.1) and (2.2) identify PH curves in \mathcal{EP}_m^ω . In order to simplify both the analysis and the construction, it is easier to identify spaces so that for every choice of the exponential polynomials a_k belonging to such spaces we can guarantee the resulting curves to be PH curves in \mathcal{EP}_m^ω .

PROPOSITION 2.4. *Let \mathcal{A}_m^ω be either $\mathcal{DEP}_{\lfloor m/2 \rfloor}^\omega$ or $\mathcal{D}^2\mathcal{OEP}_{\lfloor (m+1)/2 \rfloor}^{\omega/2}$. Then, for every $a_0, a_1, a_2, a_3 \in \mathcal{A}_m^\omega$, equation (2.2) defines a PH curve in \mathcal{EP}_m^ω .*

Proof. From (2.2), since \mathcal{DEP}_m^ω is a linear space, we only need to prove that

$$\left(\mathcal{DEP}_{\lfloor m/2 \rfloor}^\omega\right)^2 \subseteq \mathcal{DEP}_m^\omega \quad \text{and} \quad \left(\mathcal{D}^2\mathcal{OEP}_{\lfloor (m+1)/2 \rfloor}^{\omega/2}\right)^2 \subseteq \mathcal{DEP}_m^\omega.$$

Consider then, for $\alpha_k, \beta_k \in \mathbb{R}$, $k = -\lfloor m/2 \rfloor, \dots, \lfloor m/2 \rfloor$,

$$\sum_{k=-\lfloor m/2 \rfloor}^{\lfloor m/2 \rfloor} \alpha_k e^{k\omega t}, \quad \sum_{k=-\lfloor m/2 \rfloor}^{\lfloor m/2 \rfloor} \beta_k e^{k\omega t} \in \mathcal{DEP}_{\lfloor m/2 \rfloor}^\omega.$$

We have

$$\left(\sum_{k=-\lfloor m/2 \rfloor}^{\lfloor m/2 \rfloor} \alpha_k e^{k\omega t}\right) \left(\sum_{k=-\lfloor m/2 \rfloor}^{\lfloor m/2 \rfloor} \beta_k e^{k\omega t}\right) = \sum_{j,k=-\lfloor m/2 \rfloor}^{\lfloor m/2 \rfloor} \alpha_j \beta_k e^{(j+k)\omega t} \in \mathcal{DEP}_m^\omega,$$

since $-m \leq -2\lfloor m/2 \rfloor \leq j+k \leq 2\lfloor m/2 \rfloor \leq m$.

Similarly, for $\alpha_k, \beta_k \in \mathbb{R}$, $k = 1 - \lfloor (m+1)/2 \rfloor, \dots, \lfloor (m+1)/2 \rfloor$, and

$$\sum_{k=1-\lfloor (m+1)/2 \rfloor}^{\lfloor (m+1)/2 \rfloor} \alpha_k e^{\frac{2k-1}{2}\omega t}, \quad \sum_{k=1-\lfloor (m+1)/2 \rfloor}^{\lfloor (m+1)/2 \rfloor} \beta_k e^{\frac{2k-1}{2}\omega t} \in \mathcal{D}^2\mathcal{OEP}_{\lfloor (m+1)/2 \rfloor}^{\omega/2},$$

we have

$$\begin{aligned} \left(\sum_{k=1-\lfloor (m+1)/2 \rfloor}^{\lfloor (m+1)/2 \rfloor} \alpha_k e^{\frac{2k-1}{2}\omega t}\right) \left(\sum_{k=1-\lfloor (m+1)/2 \rfloor}^{\lfloor (m+1)/2 \rfloor} \beta_k e^{\frac{2k-1}{2}\omega t}\right) &= \\ &= \sum_{j,k=1-\lfloor (m+1)/2 \rfloor}^{\lfloor (m+1)/2 \rfloor} \alpha_j \beta_k e^{(j+k-1)\omega t} \in \mathcal{DEP}_m^\omega, \end{aligned}$$

since $-m \leq 1 - 2\lfloor (m+1)/2 \rfloor \leq j+k-1 \leq 2\lfloor (m+1)/2 \rfloor - 1 \leq m$. \square

Examples of major interest that we consider in the following are:

- $m = 1$: $\mathbf{r}(t)$ is a PH curve in $\mathcal{EP}_1^\omega = \text{span}\{1, t, e^{\omega t}, e^{-\omega t}\}$, its hodograph $\mathbf{r}'(t)$ is in $\mathcal{DEP}_1^\omega = \text{span}\{1, e^{\omega t}, e^{-\omega t}\}$ and \mathcal{A}_1^ω is either $\mathcal{DEP}_0^\omega = \text{span}\{1\}$ or $\mathcal{D}^2\mathcal{OEP}_1^{\omega/2} = \text{span}\{e^{\omega t/2}, e^{-\omega t/2}\}$;

- $m = 2$: $\mathbf{r}(t)$ is a PH curve in $\mathcal{EP}_2^\omega = \text{span}\{1, t, e^{\omega t}, e^{-\omega t}, e^{2\omega t}, e^{-2\omega t}\}$, its hodograph $\mathbf{r}'(t)$ is in $\mathcal{DEP}_2^\omega = \text{span}\{1, e^{\omega t}, e^{-\omega t}, e^{2\omega t}, e^{-2\omega t}\}$ and \mathcal{A}_2^ω is either $\mathcal{DEP}_1^\omega = \text{span}\{1, e^{\omega t}, e^{-\omega t}\}$ or $\mathcal{D}^2\mathcal{OEP}_1^{\omega/2} = \text{span}\{e^{\omega t/2}, e^{-\omega t/2}\}$.

For $m = 1$, $\mathcal{A}_1^\omega = \mathcal{DEP}_0^\omega$ corresponds to trivial line segments. Similarly, for $m = 2$, $\mathcal{A}_2^\omega = \mathcal{D}^2\mathcal{OEP}_1^{\omega/2}$ leads to PH curves in $\mathcal{EP}_1^\omega \subsetneq \mathcal{EP}_2^\omega$. In general, for m odd, $\mathcal{A}_m^\omega = \mathcal{DEP}_{\lfloor m/2 \rfloor}^\omega$ describes curves which actually live in $\mathcal{EP}_{m-1}^\omega$, while, for m even, this is the case for $\mathcal{A}_m^\omega = \mathcal{D}^2\mathcal{OEP}_{\lfloor (m+1)/2 \rfloor}^{\omega/2}$. Therefore, from now on we only consider

$$(2.3) \quad \mathcal{A}_m^\omega := \begin{cases} \mathcal{DEP}_{m/2}^\omega, & \text{if } m \text{ even,} \\ \mathcal{D}^2\mathcal{OEP}_{(m+1)/2}^{\omega/2}, & \text{if } m \text{ odd,} \end{cases}$$

for which $\dim(\mathcal{A}_m^\omega) = m + 1$. Starting from $\{a_k\}_{k=0}^3$ in \mathcal{A}_m^ω , (2.2) defines univocally $x'(t)$, $y'(t)$ and $z'(t)$ that belong to \mathcal{DEP}_m^ω and finally, by integration, one can obtain the analytic expressions of $x(t)$, $y(t)$ and $z(t)$ in \mathcal{EP}_m^ω . Then, for a fixed m , three spaces need to be considered. For each of these spaces a B-basis (see [8]) is defined in what follows using the notation summarized in Table 1. According to Definition 2.2,

TABLE 1
Notation used for the exponential-polynomial spaces and their respective B-basis.

space	\mathcal{A}_m^ω	\mathcal{DEP}_m^ω	\mathcal{EP}_m^ω
dimension	$m + 1$	$2m + 1$	$2(m + 1)$
B-basis	$\{\psi_{j,m}^\omega\}_{j=0}^m$	$\{\varphi_{j,m}^\omega\}_{j=0}^{2m}$	$\{\phi_{j,m}^\omega\}_{j=0}^{2m+1}$

Remark 2.3, **Proposition 2.4** and (2.3), four functions a_0, a_1, a_2, a_3 in \mathcal{A}_m^ω having no common roots define a PH curve $\mathbf{r}(t) = (x(t), y(t), z(t))$ in \mathcal{EP}_m^ω as in (2.2). Such a curve can thus be associated to a function from the interval $[0, 1]$ to the quaternions in a natural way as follows.

DEFINITION 2.5. *The function*

$$\mathbf{A}(t) := a_0(t) + a_1(t)\mathbf{i} + a_2(t)\mathbf{j} + a_3(t)\mathbf{k},$$

where $\mathbf{i}, \mathbf{j}, \mathbf{k}$ denote the so-called fundamental quaternion units (see, e.g., [3], Section 5.3), is called the preimage of $\mathbf{r}(t)$.

Expanding the coefficients of the preimage with respect to a B-basis of \mathcal{A}_m^ω as $a_k(t) = \sum_{j=0}^m a_{k,j} \psi_{j,m}^\omega(t)$, $k \in \{0, \dots, 3\}$, for some $a_{k,j} \in \mathbb{R}$, we can rewrite

$$(2.4) \quad \mathbf{A}(t) = \sum_{j=0}^m \mathbf{A}_j \psi_{j,m}^\omega(t) \quad \text{where} \quad \mathbf{A}_j = a_{0,j} + a_{1,j}\mathbf{i} + a_{2,j}\mathbf{j} + a_{3,j}\mathbf{k}.$$

Moreover, we can compactly write the hodograph $\mathbf{r}'(t) = (x'(t), y'(t), z'(t))$ of $\mathbf{r}(t)$ with the pure vector quaternion

$$(2.5) \quad \mathbf{r}'(t) = \mathbf{A}(t)\mathbf{iA}^*(t).$$

Here and in the following, with an abuse of notation, we identify vectors in \mathbb{R}^3 and pure vector quaternions via the natural bijection $(x, y, z) \longleftrightarrow x\mathbf{i} + y\mathbf{j} + z\mathbf{k}$. Accordingly, in view of (2.5), the parametric speed of $\mathbf{r}(t)$ has the quaternionic representation

$$(2.6) \quad \sigma(t) = |\mathbf{r}'(t)| = |\mathbf{A}(t)\mathbf{iA}^*(t)| = |\mathbf{A}(t)|^2 = \mathbf{A}(t)\mathbf{A}^*(t).$$

3. PH curves in \mathcal{EP}_1^ω .

3.1. The normalized B-basis of the space \mathcal{EP}_1^ω . On the interval $[0, 1]$ the non-negative exponential functions

$$(3.1) \quad \begin{aligned} \psi_{0,1}^\omega(t) &= \frac{e^{\frac{\omega}{2}(1-t)} - e^{-\frac{\omega}{2}(1-t)}}{e^{\frac{\omega}{2}} - e^{-\frac{\omega}{2}}} = \frac{\sinh(\frac{\omega}{2} - \frac{\omega}{2}t)}{\sinh(\frac{\omega}{2})}, \\ \psi_{1,1}^\omega(t) &= \frac{e^{\frac{\omega}{2}t} - e^{-\frac{\omega}{2}t}}{e^{\frac{\omega}{2}} - e^{-\frac{\omega}{2}}} = \frac{\sinh(\frac{\omega}{2}t)}{\sinh(\frac{\omega}{2})} \end{aligned}$$

define a B-basis of the extended Chebyshev space $\mathcal{A}_1^\omega = \mathcal{D}^2\mathcal{OE}\mathcal{P}_1^{\omega/2} = \text{span}\{e^{\frac{\omega}{2}t}, e^{-\frac{\omega}{2}t}\}$. However, note that $\{\psi_{0,1}^\omega(t), \psi_{1,1}^\omega(t)\}$ is not normalized since $\psi_{0,1}^\omega(t) + \psi_{1,1}^\omega(t) \neq 1$ for $t \in (0, 1)$. By squaring an arbitrary function $f \in \mathcal{A}_1^\omega$, we obtain a function f^2 that belongs to the exponential space $\mathcal{DE}\mathcal{P}_1^\omega = \text{span}\{1, e^{\omega t}, e^{-\omega t}\}$. Since we assume $\omega \in \mathbb{R}^+$, $\mathcal{DE}\mathcal{P}_1^\omega$ is an extended Chebyshev space that, on the interval $[0, 1]$, admits a normalized B-basis of the form

$$(3.2) \quad \begin{aligned} \varphi_{0,1}^\omega(t) &= \frac{(e^{\omega(1-t)} - 1)^2 e^{\omega t}}{(e^\omega - 1)^2} = \frac{\cosh(\omega - \omega t) - 1}{\cosh(\omega) - 1}, \\ \varphi_{1,1}^\omega(t) &= \frac{(e^{-\omega t} - 1)(e^{\omega t} - e^\omega)(e^\omega + 1)}{(e^\omega - 1)^2} = \frac{\cosh(\omega) - \cosh(\omega t) - \cosh(\omega - \omega t) + 1}{\cosh(\omega) - 1}, \\ \varphi_{2,1}^\omega(t) &= \frac{(e^{\omega t} - 1)^2 e^{\omega(1-t)}}{(e^\omega - 1)^2} = \frac{\cosh(\omega t) - 1}{\cosh(\omega) - 1}. \end{aligned}$$

The exponential functions $\{\varphi_{0,1}^\omega(t), \varphi_{1,1}^\omega(t), \varphi_{2,1}^\omega(t)\}$ satisfy the following relationships with the exponential functions $\{\psi_{0,1}^\omega(t), \psi_{1,1}^\omega(t)\}$:

$$(3.3) \quad \begin{aligned} \psi_{0,1}^\omega(t)^2 &= \varphi_{0,1}^\omega(t), \quad \psi_{0,1}^\omega(t) \psi_{1,1}^\omega(t) = \frac{1}{2} c_0(\omega) \varphi_{1,1}^\omega(t), \quad \psi_{1,1}^\omega(t)^2 = \varphi_{2,1}^\omega(t), \\ \text{with } c_0(\omega) &= \frac{2}{e^{\frac{\omega}{2}} + e^{-\frac{\omega}{2}}} = \frac{1}{\cosh(\frac{\omega}{2})}. \end{aligned}$$

The antiderivative of $f^2 \in \mathcal{DE}\mathcal{P}_1^\omega$ is an exponential-polynomial function that belongs to the order-4 exponential-polynomial space $\mathcal{EP}_1^\omega = \text{span}\{1, t, e^{\omega t}, e^{-\omega t}\}$. The exponential-polynomial functions

$$(3.4) \quad \begin{aligned} \phi_{0,1}^\omega(t) &= \frac{e^{\omega(1-t)} - e^{-\omega(1-t)} - 2\omega(1-t)}{e^\omega - e^{-\omega} - 2\omega} = \frac{\sinh(\omega - \omega t) - \omega(1-t)}{\sinh(\omega) - \omega}, \\ \phi_{1,1}^\omega(t) &= \frac{(e^{-\omega} - 1) \left((\omega + 1 - e^\omega) e^{\omega t} + ((\omega - 1)e^\omega + 1) e^{\omega(1-t)} \right) + (e^\omega - 1) \left(\omega(2t + (e^{-\omega} + e^\omega)(1-t)) + e^{-\omega} - e^\omega \right)}{(e^{-\omega} - 1) \left((\omega + 1 - e^\omega) e^{\omega t} + ((\omega - 1)e^\omega + 1) e^{\omega(1-t)} \right) + (e^\omega - 1) \left(\omega(2t + (e^{-\omega} + e^\omega)(1-t)) + e^{-\omega} - e^\omega \right)} \\ &= \frac{-\omega t - \omega(1-t) \cosh(\omega) + \omega \cosh(\omega - \omega t) + \sinh(\omega) - \sinh(\omega t) - \sinh(\omega - \omega t)}{(\omega \coth(\frac{\omega}{2}) - 2)(\omega - \sinh(\omega))}, \\ \phi_{2,1}^\omega(t) &= \frac{(e^{-\omega} - 1) \left((\omega + 1 - e^\omega) e^{\omega(1-t)} + ((\omega - 1)e^\omega + 1) e^{\omega t} \right) + (e^\omega - 1) \left(\omega(2(1-t) + (e^{-\omega} + e^\omega)t) + e^{-\omega} - e^\omega \right)}{(e^{-\omega} - 1) \left((\omega + 1 - e^\omega) e^{\omega(1-t)} + ((\omega - 1)e^\omega + 1) e^{\omega t} \right) + (e^\omega - 1) \left(\omega(2(1-t) + (e^{-\omega} + e^\omega)t) + e^{-\omega} - e^\omega \right)} \\ &= \frac{-\omega(1-t) - \omega t \cosh(\omega) + \omega \cosh(\omega t) + \sinh(\omega) - \sinh(\omega - \omega t) - \sinh(\omega t)}{(\omega \coth(\frac{\omega}{2}) - 2)(\omega - \sinh(\omega))}, \\ \phi_{3,1}^\omega(t) &= \frac{e^{\omega t} - e^{-\omega t} - 2\omega t}{e^\omega - e^{-\omega} - 2\omega} = \frac{\sinh(\omega t) - \omega t}{\sinh(\omega) - \omega}, \end{aligned}$$

define a normalized B-basis of the extended Chebyshev space \mathcal{EP}_1^ω on $[0, 1]$. For later use we observe that for the antiderivatives of the basis functions of $\mathcal{DE}\mathcal{P}_1^\omega$ we can write

$$(3.5) \quad \begin{aligned} \int_0^t \varphi_{0,1}^\omega(x) dx &= c_1(\omega) \phi_{0,1}^\omega(t) + (c_1(\omega) + c_2(\omega)) (\phi_{1,1}^\omega(t) + \phi_{2,1}^\omega(t) + \phi_{3,1}^\omega(t)), \\ \int_0^t \varphi_{1,1}^\omega(x) dx &= -c_1(\omega) (\phi_{0,1}^\omega(t) + \phi_{1,1}^\omega(t)) + \left(-c_1(\omega) + \frac{c_3(\omega)}{c_0(\omega)} \right) (\phi_{2,1}^\omega(t) + \phi_{3,1}^\omega(t)), \\ \int_0^t \varphi_{2,1}^\omega(x) dx &= c_2(\omega) \phi_{3,1}^\omega(t), \end{aligned}$$

with

$$(3.6) \quad c_1(\omega) = -\frac{1}{\omega} \coth\left(\frac{\omega}{2}\right), \quad c_2(\omega) = \frac{\sinh(\omega) - \omega}{\omega(\cosh(\omega) - 1)}, \quad c_3(\omega) = \frac{\frac{\omega}{2} \coth\left(\frac{\omega}{2}\right) - 1}{\frac{\omega}{2} \sinh\left(\frac{\omega}{2}\right)}.$$

3.2. Geometric properties of Bézier-like curves in \mathcal{EP}_1^ω .

DEFINITION 3.1 (Bézier-like curves in \mathcal{EP}_1^ω). *Given a control polygon with vertices $\mathbf{r}_i \in \mathbb{R}^d$, $i = 0, \dots, 3$, the associated Bézier-like curve in \mathcal{EP}_1^ω is defined as*

$$(3.7) \quad \mathbf{r}(t) = \sum_{i=0}^3 \mathbf{r}_i \phi_{i,1}^\omega(t), \quad t \in [0, 1].$$

PROPOSITION 3.2 (Properties of Bézier-like curves in \mathcal{EP}_1^ω).

The Bézier-like curve in (3.7) has the following properties:

- (a) Convex hull property and geometric invariance property. *The entire curve lies inside the convex hull of its control points and its shape is independent of the coordinate system, i.e., it is scale and translation invariant.*
- (b) Symmetry. *The control points $\mathbf{r}_0, \mathbf{r}_1, \mathbf{r}_2, \mathbf{r}_3$ and $\mathbf{r}_3, \mathbf{r}_2, \mathbf{r}_1, \mathbf{r}_0$ define the same curve with respect to different parameterizations, i.e.,*

$$\sum_{i=0}^3 \mathbf{r}_i \phi_{i,1}^\omega(t) = \sum_{i=0}^3 \mathbf{r}_{3-i} \phi_{i,1}^\omega(1-t), \quad t \in [0, 1].$$

- (c) Derivative formula.

$$\frac{d}{dt} \mathbf{r}(t) = \sum_{i=0}^2 \delta_{i,1}^\omega \Delta \mathbf{r}_i \varphi_{i,1}^\omega(t), \quad t \in [0, 1],$$

where, for all $i = 0, 1, 2$, $\Delta \mathbf{r}_i = \mathbf{r}_{i+1} - \mathbf{r}_i$ and

$$(3.8) \quad \begin{aligned} \delta_{0,1}^\omega &= 1 / \int_0^1 \varphi_{0,1}^\omega(t) dt = \frac{\omega (\cosh(\omega) - 1)}{\sinh(\omega) - \omega}, \\ \delta_{1,1}^\omega &= 1 / \int_0^1 \varphi_{1,1}^\omega(t) dt = \frac{\frac{\omega}{2} \tanh(\frac{\omega}{2})}{\frac{\omega}{2} \coth(\frac{\omega}{2}) - 1}, \\ \delta_{2,1}^\omega &= 1 / \int_0^1 \varphi_{2,1}^\omega(t) dt = \frac{\omega (\cosh(\omega) - 1)}{\sinh(\omega) - \omega}. \end{aligned}$$

- (d) Endpoint conditions.

$$\begin{aligned} \mathbf{r}(0) &= \mathbf{r}_0, & \mathbf{r}'(0) &= \delta_{0,1}^\omega (\mathbf{r}_1 - \mathbf{r}_0) = \frac{1}{c_2(\omega)} (\mathbf{r}_1 - \mathbf{r}_0), \\ \mathbf{r}(1) &= \mathbf{r}_3, & \mathbf{r}'(1) &= \delta_{2,1}^\omega (\mathbf{r}_3 - \mathbf{r}_2) = \frac{1}{c_2(\omega)} (\mathbf{r}_3 - \mathbf{r}_2). \end{aligned}$$

Proof. [Appendix A.](#) □

3.3. Control polygons of PH curves in \mathcal{EP}_1^ω . To construct a PH curve in \mathcal{EP}_1^ω , the functions a_0, a_1, a_2, a_3 are chosen in \mathcal{A}_1^ω and thus

$$a_k(t) = a_{k,0} \psi_{0,1}^\omega(t) + a_{k,1} \psi_{1,1}^\omega(t), \quad k \in \{0, \dots, 3\},$$

for some $a_{k,0}, a_{k,1} \in \mathbb{R}$. Consequently, the associated preimage is

$$(3.9) \quad \mathbf{A}(t) = \mathbf{A}_0 \psi_{0,1}^\omega(t) + \mathbf{A}_1 \psi_{1,1}^\omega(t)$$

where

$$(3.10) \quad \mathbf{A}_j = a_{0,j} \mathbf{i} + a_{1,j} \mathbf{j} + a_{2,j} \mathbf{k}, \quad j = 0, 1.$$

PROPOSITION 3.3. A PH curve $\mathbf{r}(t)$ in \mathcal{EP}_1^ω can be expressed in the Bézier-like form $\mathbf{r}(t) = \sum_{i=0}^3 \mathbf{r}_i \phi_{i,1}^\omega(t)$, with Bézier-like control points \mathbf{r}_i , $i = 1, \dots, 3$ given in terms of the freely chosen integration constant \mathbf{r}_0 , of the numbers in (3.6) and of the coefficients of the preimage $\mathbf{A}(t)$ in (3.9) and (3.10) by

$$(3.11) \quad \begin{aligned} \mathbf{r}_1 &= \mathbf{r}_0 + c_2(\omega) \mathbf{A}_0 \mathbf{i} \mathbf{A}_0^*, & \mathbf{r}_2 &= \mathbf{r}_1 + c_3(\omega) \frac{1}{2} (\mathbf{A}_0 \mathbf{i} \mathbf{A}_1^* + \mathbf{A}_1 \mathbf{i} \mathbf{A}_0^*), \\ \mathbf{r}_3 &= \mathbf{r}_2 + c_2(\omega) \mathbf{A}_1 \mathbf{i} \mathbf{A}_1^*. \end{aligned}$$

Proof. Appendix B. □

Remark 3.4. Since, from (3.6), $\lim_{\omega \rightarrow 0} c_2(\omega) = \lim_{\omega \rightarrow 0} c_3(\omega) = 1/3$, (3.11) recover the well-known results of the cubic polynomial case when $\omega \rightarrow 0$, see [3].

3.4. Parametric speed, cumulative and total arc length in \mathcal{EP}_1^ω .

PROPOSITION 3.5. The parametric speed of $\mathbf{r}(t)$ is a function in \mathcal{DEP}_1^ω with the explicit expression $\sigma(t) = \sum_{i=0}^2 \sigma_i \phi_{i,1}^\omega(t)$, where

$$(3.12) \quad \sigma_0 = |\mathbf{A}_0|^2, \quad \sigma_1 = c_0(\omega) \frac{1}{2} (\mathbf{A}_1 \mathbf{A}_0^* + \mathbf{A}_0 \mathbf{A}_1^*), \quad \sigma_2 = |\mathbf{A}_1|^2.$$

Proof. Appendix C. □

PROPOSITION 3.6. The arc length function of $\mathbf{r}(t)$ is a function in \mathcal{EP}_1^ω having the expression $s(t) = \sum_{i=0}^3 s_i \phi_{i,1}^\omega(t)$, where

$$s_0 = (\sigma_0 - \sigma_1) c_1(\omega), \quad s_1 = s_0 + \sigma_0 c_2(\omega), \quad s_2 = s_1 + \sigma_1 \frac{c_3(\omega)}{c_0(\omega)}, \quad s_3 = s_2 + \sigma_2 c_2(\omega).$$

Proof. Appendix D. □

COROLLARY 3.7. For a given $\xi \in [0, 1]$, the cumulative arc length of $\mathbf{r}(t)$ is

$$\begin{aligned} S(\xi) &= s(\xi) - s(0) = \sum_{i=0}^3 s_i (\phi_{i,1}^\omega(\xi) - \phi_{i,1}^\omega(0)) \\ &= s_0 (\phi_{0,1}^\omega(\xi) - 1) + s_1 \phi_{1,1}^\omega(\xi) + s_2 \phi_{2,1}^\omega(\xi) + s_3 \phi_{3,1}^\omega(\xi) \end{aligned}$$

and, exploiting the properties of the normalized B-basis $\{\phi_{i,1}^\omega\}_{i=0}^3$ at 0 and 1 (see [12, equations (6)-(8)]), the total arc length assumes the simplified expression

$$(3.13) \quad \begin{aligned} S(1) &= s_3 - s_0 = (\sigma_0 + \sigma_2) c_2(\omega) + \sigma_1 \frac{c_3(\omega)}{c_0(\omega)} \\ &= c_2(\omega) (|\mathbf{A}_0|^2 + |\mathbf{A}_1|^2) + c_3(\omega) \frac{1}{2} (\mathbf{A}_1 \mathbf{A}_0^* + \mathbf{A}_0 \mathbf{A}_1^*). \end{aligned}$$

Remark 3.8. When $\omega \rightarrow 0$, the total arc length formula in (3.13) yields $S(1) = (|\mathbf{A}_0|^2 + |\mathbf{A}_1|^2)/3 + (\mathbf{A}_1 \mathbf{A}_0^* + \mathbf{A}_0 \mathbf{A}_1^*)/6$, thus recovering the well-known result of the cubic polynomial case [3].

4. PH curves in \mathcal{EP}_2^ω .

4.1. The normalized B-basis of the space \mathcal{EP}_2^ω . By squaring an arbitrary function $f \in \mathcal{A}_2^\omega = \text{span}\{1, e^{\omega t}, e^{-\omega t}\}$, we obtain a function f^2 that belongs to the exponential space $\mathcal{DEP}_2^\omega = \text{span}\{1, e^{\omega t}, e^{-\omega t}, e^{2\omega t}, e^{-2\omega t}\}$. Since $\mathcal{A}_2^\omega = \mathcal{DEP}_1^\omega$ we

can choose $\psi_{j,2}^\omega(t) = \varphi_{j,1}^\omega(t)$, $j \in \{0, 1, 2\}$ as in (3.2). Then, \mathcal{DEP}_2^ω is an extended Chebyshev space that, on the interval $[0, 1]$, admits a normalized B-basis of the form

$$\begin{aligned}\varphi_{0,2}^\omega(t) &= \psi_{0,2}^\omega(t)^2, & \varphi_{1,2}^\omega(t) &= 2\psi_{0,2}^\omega(t)\psi_{1,2}^\omega(t), \\ \varphi_{2,2}^\omega(t) &= \psi_{1,2}^\omega(t)^2 + 2\psi_{0,2}^\omega(t)\psi_{2,2}^\omega(t), \\ \varphi_{3,2}^\omega(t) &= 2\psi_{1,2}^\omega(t)\psi_{2,2}^\omega(t), & \varphi_{4,2}^\omega(t) &= \psi_{2,2}^\omega(t)^2.\end{aligned}$$

The inverse relationship between the exponential functions $\{\varphi_{j,2}^\omega(t)\}_{j=0}^4$ and the exponential functions $\{\psi_{j,2}^\omega(t)\}_{j=0}^2$ is instead given by

$$(4.1) \quad \begin{aligned}\psi_{0,2}^\omega(t)^2 &= \varphi_{0,2}^\omega(t), & \psi_{0,2}^\omega(t)\psi_{1,2}^\omega(t) &= \frac{1}{2}\varphi_{1,2}^\omega(t), \\ \psi_{1,2}^\omega(t)^2 &= q_0(\omega)\varphi_{2,2}^\omega(t), & \psi_{0,2}^\omega(t)\psi_{2,2}^\omega(t) &= \frac{1}{2}q_1(\omega)\varphi_{2,2}^\omega(t), \\ \psi_{1,2}^\omega(t)\psi_{2,2}^\omega(t) &= \frac{1}{2}\varphi_{3,2}^\omega(t), & \psi_{2,2}^\omega(t)^2 &= \varphi_{4,2}^\omega(t),\end{aligned}$$

with $q_0(\omega) = \frac{\cosh(\omega)+1}{\cosh(\omega)+2}$, $q_1(\omega) = \frac{1}{\cosh(\omega)+2}$.

The antiderivative of a function in \mathcal{DEP}_2^ω is an exponential-polynomial function that belongs to the order-6 exponential-polynomial space \mathcal{EP}_2^ω . The exponential-polynomial functions

$$(4.2) \quad \begin{aligned}\phi_{0,2}^\omega(t) &= \frac{g_0(\omega-\omega t)}{g_0(\omega)}, & \phi_{1,2}^\omega(t) &= g_1(\omega) \sinh\left(\frac{\omega}{2}\right) \left(\sinh^4\left(\frac{\omega-\omega t}{2}\right) - \sinh^4\left(\frac{\omega}{2}\right) \frac{g_0(\omega-\omega t)}{g_0(\omega)} \right), \\ \phi_{2,2}^\omega(t) &= g_2(\omega) \left(-16 \sinh^3\left(\frac{\omega-\omega t}{2}\right) \sinh\left(\frac{\omega t}{2}\right) + g_1(\omega)g_0(\omega) \sinh^4\left(\frac{\omega-\omega t}{2}\right) - g_1(\omega) \sinh^4\left(\frac{\omega}{2}\right) g_0(\omega-\omega t) \right), \\ \phi_{3,2}^\omega(t) &= g_2(\omega) \left(-16 \sinh^3\left(\frac{\omega t}{2}\right) \sinh\left(\frac{\omega-\omega t}{2}\right) + g_1(\omega)g_0(\omega) \sinh^4\left(\frac{\omega t}{2}\right) - g_1(\omega) \sinh^4\left(\frac{\omega}{2}\right) g_0(\omega t) \right), \\ \phi_{4,2}^\omega(t) &= g_1(\omega) \sinh\left(\frac{\omega}{2}\right) \left(\sinh^4\left(\frac{\omega t}{2}\right) - \sinh^4\left(\frac{\omega}{2}\right) \frac{g_0(\omega t)}{g_0(\omega)} \right), & \phi_{5,2}^\omega(t) &= \frac{g_0(\omega t)}{g_0(\omega)},\end{aligned}$$

with

$$\begin{aligned}g_0(\omega) &= 3\omega + \sinh(\omega)(\cosh(\omega) - 4), & g_1(\omega) &= \frac{4}{\sinh\left(\frac{\omega}{2}\right)(\cosh(\omega) - 3\omega \coth\left(\frac{\omega}{2}\right) + 5)}, \\ g_2(\omega) &= \frac{\sinh\left(\frac{\omega}{2}\right)}{3(3 \sinh(\omega) - \omega(\cosh(\omega) + 2))},\end{aligned}$$

define a normalized B-basis of the extended Chebyshev space \mathcal{EP}_2^ω on $[0, 1]$. For later use we observe that for the antiderivatives of the basis functions of \mathcal{DEP}_2^ω we can write

$$(4.3) \quad \begin{aligned}\int_0^t \varphi_{0,2}^\omega(x) dx &= p_0(\omega)\phi_{0,2}^\omega(t) + (p_0(\omega) + q_2(\omega)) \sum_{i=1}^5 \phi_{i,2}^\omega(t), \\ \int_0^t \varphi_{1,2}^\omega(x) dx &= p_1(\omega)(\phi_{0,2}^\omega(t) + \phi_{1,2}^\omega(t)) + (p_1(\omega) + q_3(\omega)) \sum_{i=2}^5 \phi_{i,2}^\omega(t), \\ \int_0^t \varphi_{2,2}^\omega(x) dx &= p_2(\omega) \sum_{i=0}^2 \phi_{i,2}^\omega(t) + \left(p_2(\omega) + \frac{q_4(\omega)}{q_1(\omega)} \right) \sum_{i=3}^5 \phi_{i,2}^\omega(t), \\ \int_0^t \varphi_{3,2}^\omega(x) dx &= p_3(\omega) \sum_{i=0}^3 \phi_{i,2}^\omega(t) + (p_3(\omega) + q_3(\omega)) (\phi_{4,2}^\omega(t) + \phi_{5,2}^\omega(t)), \\ \int_0^t \varphi_{4,2}^\omega(x) dx &= q_2(\omega)\phi_{5,2}^\omega(t),\end{aligned}$$

with

$$(4.4) \quad \begin{aligned}p_0(\omega) &= -\frac{\sinh(\omega)(\cosh(\omega)-4)}{2\omega(\cosh(\omega)-1)^2}, & p_1(\omega) &= -\frac{\sinh(\omega)(2\cosh(\omega)+7)}{2\omega(\cosh(\omega)-1)^2}, \\ p_2(\omega) &= \frac{3\sinh(\omega)(\cosh(\omega)+2)}{2\omega(\cosh(\omega)-1)^2}, & p_3(\omega) &= -\frac{\sinh(\omega)}{\omega(\cosh(\omega)-1)^2},\end{aligned}$$

and

$$(4.5) \quad \begin{aligned} q_2(\omega) &= \frac{g_0(\omega)}{2\omega(\cosh(\omega)-1)^2}, & q_3(\omega) &= \frac{5\sinh(\omega)-3\omega+(\sinh(\omega)-3\omega)\cosh(\omega)}{\omega(\cosh(\omega)-1)^2}, \\ q_4(\omega) &= \frac{\omega(2+\cosh(\omega))-3\sinh(\omega)}{\omega(\cosh(\omega)-1)^2}. \end{aligned}$$

4.2. Geometric properties of Bézier-like curves in \mathcal{EP}_2^ω .

DEFINITION 4.1 (Bézier-like curves in \mathcal{EP}_2^ω). *Given a control polygon with vertices $\mathbf{r}_i \in \mathbb{R}^d$, $i = 0, \dots, 5$, the associated Bézier-like curve in \mathcal{EP}_2^ω is defined as*

$$(4.6) \quad \mathbf{r}(t) = \sum_{i=0}^5 \mathbf{r}_i \phi_{i,2}^\omega(t), \quad t \in [0, 1].$$

PROPOSITION 4.2 (Properties of Bézier-like curves in \mathcal{EP}_2^ω).

The Bézier-like curve in (4.6) has the following properties:

- (a) Convex hull property and geometric invariance property. *The entire curve lies inside the convex hull of its control points and its shape is independent of the coordinate system, i.e., it is scale and translation invariant.*
- (b) Symmetry. *The control points $\mathbf{r}_0, \mathbf{r}_1, \dots, \mathbf{r}_5$ and $\mathbf{r}_5, \dots, \mathbf{r}_1, \mathbf{r}_0$ define the same curve with respect to different parameterizations, i.e.,*

$$\sum_{i=0}^5 \mathbf{r}_i \phi_{i,2}^\omega(t) = \sum_{i=0}^5 \mathbf{r}_{5-i} \phi_{i,2}^\omega(1-t), \quad t \in [0, 1].$$

- (c) Derivative formula.

$$\frac{d}{dt} \mathbf{r}(t) = \sum_{i=0}^4 \epsilon_{i,2}^\omega \Delta \mathbf{r}_i \varphi_{i,2}^\omega(t), \quad t \in [0, 1],$$

where, for all $i = 0, \dots, 4$, $\Delta \mathbf{r}_i = \mathbf{r}_{i+1} - \mathbf{r}_i$ and $\epsilon_{i,2}^\omega$ are given by

$$(4.7) \quad \begin{aligned} \epsilon_{0,2}^\omega &= 1 / \int_0^1 \varphi_{0,2}^\omega(t) dt = \frac{4\omega(\cosh(\omega)-1)^2}{6\omega + \sinh(2\omega) - 8\sinh(\omega)}, \\ \epsilon_{1,2}^\omega &= 1 / \int_0^1 \varphi_{1,2}^\omega(t) dt = \frac{\omega(\cosh(\omega)-1)^2}{5\sinh(\omega) - \cosh(\omega)(3\omega - \sinh(\omega)) - 3\omega}, \\ \epsilon_{2,2}^\omega &= 1 / \int_0^1 \varphi_{2,2}^\omega(t) dt = \frac{\omega(\cosh(\omega)-1)^2}{(\cosh(\omega)+2)(2\omega + \omega\cosh(\omega) - 3\sinh(\omega))}, \\ \epsilon_{3,2}^\omega &= 1 / \int_0^1 \varphi_{3,2}^\omega(t) dt = \frac{\omega(\cosh(\omega)-1)^2}{5\sinh(\omega) - \cosh(\omega)(3\omega - \sinh(\omega)) - 3\omega}, \\ \epsilon_{4,2}^\omega &= 1 / \int_0^1 \varphi_{4,2}^\omega(t) dt = \frac{4\omega(\cosh(\omega)-1)^2}{6\omega + \sinh(2\omega) - 8\sinh(\omega)}. \end{aligned}$$

- (d) Endpoint conditions.

$$\begin{aligned} \mathbf{r}(0) &= \mathbf{r}_0, & \mathbf{r}'(0) &= \epsilon_{0,2}^\omega (\mathbf{r}_1 - \mathbf{r}_0) = \frac{1}{q_2(\omega)} (\mathbf{r}_1 - \mathbf{r}_0), \\ \mathbf{r}(1) &= \mathbf{r}_5, & \mathbf{r}'(1) &= \epsilon_{4,2}^\omega (\mathbf{r}_5 - \mathbf{r}_4) = \frac{1}{q_2(\omega)} (\mathbf{r}_5 - \mathbf{r}_4). \end{aligned}$$

Proof. [Appendix E](#). □

4.3. **Control polygons of PH curves in \mathcal{EP}_2^ω .** To construct a spatial PH curve in \mathcal{EP}_2^ω , the functions a_0, a_1, a_2, a_3 are chosen in \mathcal{A}_2^ω and thus $a_k(t) = \sum_{j=0}^2 a_{k,j} \psi_{j,2}^\omega(t)$, $k \in \{0, \dots, 3\}$, for some $a_{k,j} \in \mathbb{R}$. Consequently, the associated preimage is

$$(4.8) \quad \mathbf{A}(t) = \sum_{j=0}^2 \mathbf{A}_j \psi_{j,2}^\omega(t)$$

where

$$(4.9) \quad \mathbf{A}_j = a_{0,j} \mathbf{i} + a_{1,j} \mathbf{j} + a_{2,j} \mathbf{k}, \quad j = 0, 1, 2.$$

PROPOSITION 4.3. *A PH curve $\mathbf{r}(t)$ in \mathcal{EP}_2^ω can be expressed in the Bézier-like form $\mathbf{r}(t) = \sum_{i=0}^5 \mathbf{r}_i \phi_{i,2}^\omega(t)$, with Bézier-like control points \mathbf{r}_i , $i = 1, \dots, 5$ given in terms of the freely chosen integration constant \mathbf{r}_0 , of the numbers in (4.1) and (4.5) and of the coefficients of the preimage $\mathbf{A}(t)$ in (4.8) and (4.9) by*

$$(4.10) \quad \begin{aligned} \mathbf{r}_1 &= \mathbf{r}_0 + q_2(\omega) \mathbf{A}_0 \mathbf{i} \mathbf{A}_0^*, & \mathbf{r}_2 &= \mathbf{r}_1 + q_3(\omega) \frac{1}{2} (\mathbf{A}_0 \mathbf{i} \mathbf{A}_1^* + \mathbf{A}_1 \mathbf{i} \mathbf{A}_0^*), \\ \mathbf{r}_3 &= \mathbf{r}_2 + q_4(\omega) \left(\frac{1}{2} (\mathbf{A}_0 \mathbf{i} \mathbf{A}_2^* + \mathbf{A}_2 \mathbf{i} \mathbf{A}_0^*) + \frac{q_0(\omega)}{q_1(\omega)} \mathbf{A}_1 \mathbf{i} \mathbf{A}_1^* \right), \\ \mathbf{r}_4 &= \mathbf{r}_3 + q_3(\omega) \frac{1}{2} (\mathbf{A}_1 \mathbf{i} \mathbf{A}_2^* + \mathbf{A}_2 \mathbf{i} \mathbf{A}_1^*), & \mathbf{r}_5 &= \mathbf{r}_4 + q_2(\omega) \mathbf{A}_2 \mathbf{i} \mathbf{A}_2^*. \end{aligned}$$

Proof. Appendix F. □

Remark 4.4. Since, from (4.1) and (4.5),

$$\lim_{\omega \rightarrow 0} \frac{q_0(\omega)}{q_1(\omega)} = 2, \quad \lim_{\omega \rightarrow 0} q_2(\omega) = \lim_{\omega \rightarrow 0} q_3(\omega) = \frac{1}{5} \quad \text{and} \quad \lim_{\omega \rightarrow 0} q_4(\omega) = \frac{1}{15},$$

(4.10) recover the well-known results of the quintic polynomial case when $\omega \rightarrow 0$, see [3].

4.4. Parametric speed, cumulative and total arc length in \mathcal{EP}_2^ω .

PROPOSITION 4.5. *The parametric speed of $\mathbf{r}(t)$ is a function in \mathcal{DEP}_2^ω having the expression $\sigma(t) = \sum_{i=0}^4 \sigma_i \phi_{i,2}^\omega(t)$, where*

$$(4.11) \quad \begin{aligned} \sigma_0 &= |\mathbf{A}_0|^2, & \sigma_1 &= \frac{1}{2} (\mathbf{A}_1 \mathbf{A}_0^* + \mathbf{A}_0 \mathbf{A}_1^*), \\ \sigma_2 &= q_0(\omega) |\mathbf{A}_1|^2 + q_1(\omega) \frac{1}{2} (\mathbf{A}_2 \mathbf{A}_0^* + \mathbf{A}_0 \mathbf{A}_2^*), \\ \sigma_3 &= \frac{1}{2} (\mathbf{A}_1 \mathbf{A}_2^* + \mathbf{A}_2 \mathbf{A}_1^*), & \sigma_4 &= |\mathbf{A}_2|^2. \end{aligned}$$

Proof. Appendix G. □

PROPOSITION 4.6. *The arc length function of $\mathbf{r}(t)$ is a function in \mathcal{EP}_2^ω having the expression $s(t) = \sum_{i=0}^5 s_i \phi_{i,2}^\omega(t)$, where*

$$\begin{aligned} s_0 &= \sum_{j=0}^3 \sigma_j p_j(\omega), & s_1 &= s_0 + \sigma_0 q_2(\omega), & s_2 &= s_1 + \sigma_1 q_3(\omega), \\ s_3 &= s_2 + \sigma_2 \frac{q_4(\omega)}{q_1(\omega)}, & s_4 &= s_3 + \sigma_3 q_3(\omega), & s_5 &= s_4 + \sigma_4 q_2(\omega). \end{aligned}$$

Proof. Appendix H. □

COROLLARY 4.7. *For a given $\xi \in [0, 1]$, the cumulative arc length of $\mathbf{r}(t)$ is*

$$S(\xi) = s(\xi) - s(0) = \sum_{i=0}^5 s_i (\phi_{i,2}^\omega(\xi) - \phi_{i,2}^\omega(0))$$

and, exploiting the properties of the normalized B-basis $\{\phi_{i,2}^\omega\}_{i=0}^5$ at 0 and 1 (see [12, equations (6)-(8)]), the total arc length assumes the simplified expression

$$\begin{aligned}
 S(1) &= s_5 - s_0 = (\sigma_0 + \sigma_4)q_2(\omega) + (\sigma_1 + \sigma_3)q_3(\omega) + \sigma_2 \frac{q_4(\omega)}{q_1(\omega)} \\
 (4.12) \quad &= q_2(\omega)(|\mathbf{A}_0|^2 + |\mathbf{A}_2|^2) + q_4(\omega) \frac{q_0(\omega)}{q_1(\omega)} |\mathbf{A}_1|^2 + q_3(\omega) \frac{1}{2} (\mathbf{A}_1 \mathbf{A}_0^* + \mathbf{A}_0 \mathbf{A}_1^*) \\
 &\quad + q_3(\omega) \frac{1}{2} (\mathbf{A}_1 \mathbf{A}_2^* + \mathbf{A}_2 \mathbf{A}_1^*) + q_4(\omega) \frac{1}{2} (\mathbf{A}_2 \mathbf{A}_0^* + \mathbf{A}_0 \mathbf{A}_2^*).
 \end{aligned}$$

Remark 4.8. When $\omega \rightarrow 0$, the total arc length formula in (4.12) yields

$$\begin{aligned}
 S(1) &= \frac{1}{5} (|\mathbf{A}_0|^2 + |\mathbf{A}_2|^2) + \frac{2}{15} |\mathbf{A}_1|^2 + \frac{1}{10} (\mathbf{A}_1 \mathbf{A}_0^* + \mathbf{A}_0 \mathbf{A}_1^*) \\
 &\quad + \frac{1}{10} (\mathbf{A}_1 \mathbf{A}_2^* + \mathbf{A}_2 \mathbf{A}_1^*) + \frac{1}{30} (\mathbf{A}_2 \mathbf{A}_0^* + \mathbf{A}_0 \mathbf{A}_2^*),
 \end{aligned}$$

thus recovering the well-known result of the quintic polynomial case, see [3].

5. First-order Hermite interpolation by EPH curves. PH curves in \mathcal{EP}_2^ω are of great practical interest since they are the simplest EPH curves that can match first-order Hermite data. The problem of interpolating first-order Hermite data consists in constructing EPH curves that interpolate prescribed end points $\mathbf{r}_0, \mathbf{r}_5$ and first derivatives at these end points, hereinafter denoted by $\mathbf{d}_i, \mathbf{d}_f$, respectively. For the sake of conciseness, we also introduce the following abbreviations that do not specify the dependence on ω :

$$I_0 := q_2(\omega), \quad I_1 := \frac{1}{2} q_3(\omega), \quad I_2 := \frac{1}{2} q_4(\omega), \quad I_3 := \frac{q_0(\omega)}{q_1(\omega)} q_4(\omega).$$

PROPOSITION 5.1. *The PH curves $\mathbf{r}(t)$ in \mathcal{EP}_2^ω solving the first-order Hermite interpolation problem $\mathbf{r}(0) = \mathbf{r}_0$, $\mathbf{r}'(0) = \mathbf{d}_i$, $\mathbf{r}(1) = \mathbf{r}_5$, $\mathbf{r}'(1) = \mathbf{d}_f$, have control points given by (4.10) with*

$$\begin{aligned}
 (5.1) \quad \mathbf{A}_0 &= \sqrt{|\mathbf{d}_i|} \frac{\mathbf{i} + \mathbf{w}_i}{|\mathbf{i} + \mathbf{w}_i|} \exp(\eta_0 \mathbf{i}), \quad \mathbf{A}_2 = \sqrt{|\mathbf{d}_f|} \frac{\mathbf{i} + \mathbf{w}_f}{|\mathbf{i} + \mathbf{w}_f|} \exp(\eta_2 \mathbf{i}), \\
 \mathbf{A}_1 &= -\frac{I_1}{I_3} (\mathbf{A}_0 + \mathbf{A}_2) + \frac{\sqrt{|c|}}{I_3} \frac{\mathbf{i} + \mathbf{w}_c}{|\mathbf{i} + \mathbf{w}_c|} \exp(\eta_1 \mathbf{i}),
 \end{aligned}$$

where

$$(5.2) \quad \mathbf{c} := I_3 (\mathbf{r}_5 - \mathbf{r}_0) + (I_1^2 - I_0 I_3) (\mathbf{d}_i + \mathbf{d}_f) + (I_1^2 - I_2 I_3) (\mathbf{A}_0 \mathbf{i} \mathbf{A}_2^* + \mathbf{A}_2 \mathbf{i} \mathbf{A}_0^*),$$

and

- $(\lambda_i, \mu_i, \nu_i), (\lambda_f, \mu_f, \nu_f), (\lambda_c, \mu_c, \nu_c)$ are the direction cosines of $\mathbf{d}_i, \mathbf{d}_f$ and \mathbf{c} , respectively;
- $\mathbf{w}_i = \lambda_i \mathbf{i} + \mu_i \mathbf{j} + \nu_i \mathbf{k}$, $\mathbf{w}_f = \lambda_f \mathbf{i} + \mu_f \mathbf{j} + \nu_f \mathbf{k}$, $\mathbf{w}_c = \lambda_c \mathbf{i} + \mu_c \mathbf{j} + \nu_c \mathbf{k}$ are unit vectors in the directions of $\mathbf{d}_i, \mathbf{d}_f$ and \mathbf{c} , respectively;
- η_0, η_1, η_2 are free angular variables in $[-\pi/2, \pi/2]$.

Proof. In view of (2.5) and (4.8), interpolation of the end-derivatives yields the equations

$$(5.3) \quad \mathbf{A}_0 \mathbf{i} \mathbf{A}_0^* = \mathbf{d}_i, \quad \mathbf{A}_2 \mathbf{i} \mathbf{A}_2^* = \mathbf{d}_f,$$

for \mathbf{A}_0 and \mathbf{A}_2 , where \mathbf{d}_i and \mathbf{d}_f are known pure vector quaternions. Moreover, interpolation of the end points \mathbf{r}_0 and \mathbf{r}_5 gives the condition

$$(5.4) \quad \begin{aligned} \int_0^1 \mathbf{A}(t) \mathbf{i} \mathbf{A}^*(t) dt &= \mathbf{r}_5 - \mathbf{r}_0 \\ &= I_0 \mathbf{A}_0 \mathbf{i} \mathbf{A}_0^* + I_1 (\mathbf{A}_0 \mathbf{i} \mathbf{A}_1^* + \mathbf{A}_1 \mathbf{i} \mathbf{A}_0^*) + I_2 (\mathbf{A}_0 \mathbf{i} \mathbf{A}_2^* + \mathbf{A}_2 \mathbf{i} \mathbf{A}_0^*) \\ &\quad + I_3 \mathbf{A}_1 \mathbf{i} \mathbf{A}_1^* + I_1 (\mathbf{A}_1 \mathbf{i} \mathbf{A}_2^* + \mathbf{A}_2 \mathbf{i} \mathbf{A}_1^*) + I_0 \mathbf{A}_2 \mathbf{i} \mathbf{A}_2^*. \end{aligned}$$

Recalling the result in [4, Section 3.2], the quaternion equations (5.3) can be solved directly obtaining

$$(5.5) \quad \mathbf{A}_0 = \sqrt{|\mathbf{d}_i|} \frac{\mathbf{i} + \mathbf{w}_i}{|\mathbf{i} + \mathbf{w}_i|} \exp(\eta_0 \mathbf{i}) \quad \text{and} \quad \mathbf{A}_2 = \sqrt{|\mathbf{d}_f|} \frac{\mathbf{i} + \mathbf{w}_f}{|\mathbf{i} + \mathbf{w}_f|} \exp(\eta_2 \mathbf{i}).$$

Knowing \mathbf{A}_0 and \mathbf{A}_2 , the solution of (5.4) for \mathbf{A}_1 may appear more difficult. However, by using (5.3) and making appropriate rearrangements, (5.4) can be rewritten as

$$(5.6) \quad \begin{aligned} (I_1 \mathbf{A}_0 + I_3 \mathbf{A}_1 + I_1 \mathbf{A}_2) \mathbf{i} (I_1 \mathbf{A}_0 + I_3 \mathbf{A}_1 + I_1 \mathbf{A}_2)^* &= \\ &= I_3 (\mathbf{r}_5 - \mathbf{r}_0) + (I_1^2 - I_0 I_3) (\mathbf{d}_i + \mathbf{d}_f) + (I_1^2 - I_2 I_3) (\mathbf{A}_0 \mathbf{i} \mathbf{A}_2^* + \mathbf{A}_2 \mathbf{i} \mathbf{A}_0^*). \end{aligned}$$

Equation (5.6) is of the form $\widehat{\mathbf{A}} \mathbf{i} \widehat{\mathbf{A}}^* = \mathbf{c}$ (exactly as (5.3)) where

$$(5.7) \quad \widehat{\mathbf{A}} := I_1 \mathbf{A}_0 + I_3 \mathbf{A}_1 + I_1 \mathbf{A}_2.$$

Note that \mathbf{c} is a known pure vector quaternion. Exploiting (5.5) we can write

$$\mathbf{A}_0 \mathbf{i} \mathbf{A}_2^* + \mathbf{A}_2 \mathbf{i} \mathbf{A}_0^* = \sqrt{(1 + \lambda_i) |\mathbf{d}_i| (1 + \lambda_f) |\mathbf{d}_f|} (a_x \mathbf{i} + a_y \mathbf{j} + a_z \mathbf{k}),$$

where

$$\begin{aligned} a_x &= \cos(\Delta\eta) - \frac{(\mu_i \mu_f + \nu_i \nu_f) \cos(\Delta\eta) + (\mu_i \nu_f - \mu_f \nu_i) \sin(\Delta\eta)}{(1 + \lambda_i)(1 + \lambda_f)}, \\ a_y &= \frac{\mu_i \cos(\Delta\eta) - \nu_i \sin(\Delta\eta)}{1 + \lambda_i} + \frac{\mu_f \cos(\Delta\eta) + \nu_f \sin(\Delta\eta)}{1 + \lambda_f}, \\ a_z &= \frac{\nu_i \cos(\Delta\eta) + \mu_i \sin(\Delta\eta)}{1 + \lambda_i} + \frac{\nu_f \cos(\Delta\eta) - \mu_f \sin(\Delta\eta)}{1 + \lambda_f}, \end{aligned}$$

with $\Delta\eta := \eta_2 - \eta_0$. Finally, writing $\mathbf{c} = c_x \mathbf{i} + c_y \mathbf{j} + c_z \mathbf{k}$, the solution of (5.6) for \mathbf{A}_1 is

$$\mathbf{A}_1 = -\frac{I_1}{I_3} (\mathbf{A}_0 + \mathbf{A}_2) + \frac{\sqrt{|\mathbf{c}|}}{I_3} \frac{\mathbf{i} + \mathbf{w}_c}{|\mathbf{i} + \mathbf{w}_c|} \exp(\eta_1 \mathbf{i}),$$

which concludes the proof. \square

An example about the application of [Proposition 5.1](#) for planar Hermite data is shown in [Figure 2](#).

Remark 5.2. When $\omega \rightarrow 0$ the result of [Proposition 5.1](#) gets back the well-known result of the quintic polynomial case treated in [4].

6. Evaluation of EPH curves. In order to evaluate EPH curves two considerations have to be done. On the one hand, looking at the expressions of the normalized B-basis (3.4) and (4.2), it is clear that they are not suited for computations when ω is large. The strategy to avoid this problem is to express all the functions involved as a ratio of exponential polynomials, simplifying the dominant growth term. Unfortunately, the resulting expressions are very long. For this reason they are not presented here, but they can be found in [Appendix J](#).

On the other hand, computational problems also arise for small values of ω . Unfortunately, this issue cannot be solved like the previous one with an analytic trick. A way to proceed in this case is to consider for each basis function $\phi_{i,m}^\omega(t)$ its corresponding Taylor expansion $T_{i,m}^\omega(t)$ at $\omega = 0$ up to a certain order, and then to rely on an efficient algorithm for polynomial evaluation. This is a fair strategy, even from a theoretical point of view, since, for $\omega \rightarrow 0$, the considered EPH spaces become exactly polynomial spaces. In our numerical computations we considered 5th order Taylor expansions which, for completeness, can be found in [Appendix I](#).

Here we propose a new ad hoc point-wise evaluation algorithm and we compare it with the de Casteljaeu-like B-algorithm [7] and the recent method proposed by Woźny and Chudy in [13]. For the sake of brevity, we only provide a sketch of these two algorithms in [Algorithm 6.1](#) and [Algorithm 6.2](#), where the auxiliary functions $\lambda_{i,j,m}^\omega$ and $h_{j,m}^\omega$ are constructed following the strategies detailed in [7] and [13], respectively. In order to implement the methods, we recall that all the functions involved must be rewritten in a stable form as the basis functions in [Appendix J](#).

Each of these methods has a different running time and a different behavior as ω approaches 0. As it is shown in this section, the newly proposed algorithm yields the best results on both fronts and therefore we suggest it as the go-to evaluation algorithm for EPH curves.

Algorithm 6.1 de Casteljaeu-like

```

Acquire  $\mathbf{r}_0^0 := \mathbf{r}_0, \mathbf{r}_1^0 := \mathbf{r}_1, \dots, \mathbf{r}_{2m+1}^0 := \mathbf{r}_{2m+1}, \hat{t}$ 
for  $k = 1, \dots, 2m + 1$  do
  for  $i = 0, \dots, 2m + 1 - k$  do
     $\mathbf{r}_i^k \leftarrow (1 - \lambda_{i,2m+1-k,m}^\omega(\hat{t})) \mathbf{r}_i^{k-1} + \lambda_{i,2m+1-k,m}^\omega(\hat{t}) \mathbf{r}_{i+1}^{k-1}$ 
  end for
end for
return  $\mathbf{r}_0^{2m+1}$ 

```

Algorithm 6.2 Woźny-Chudy

```

Acquire  $\mathbf{q}_0 := \mathbf{r}_0, \mathbf{r}_1, \dots, \mathbf{r}_{2m+1}, \hat{t}$ 
for  $k = 1, \dots, 2m + 1$  do
   $\mathbf{q}_k \leftarrow (1 - h_{2m+1-k,m}^\omega(\hat{t})) \mathbf{q}_{k-1} + h_{2m+1-k,m}^\omega(\hat{t}) \mathbf{r}_k$ 
end for
return  $\mathbf{q}_{2m+1}$ 

```

We recall that, fixed $d \in \{2, 3\}$ and $m \in \{1, 2\}$, our interest here is to evaluate the curve $\mathbf{r}(t) = \sum_{i=0}^{2m+1} \mathbf{r}_i \phi_{i,m}^\omega(t)$, at a given $\hat{t} \in [0, 1]$, for a set of control points $\mathbf{r}_i \in \mathbb{R}^d$, $i = 0, \dots, 2m + 1$. The de Casteljaeu's algorithm finds the value of $\mathbf{r}(\hat{t})$ computing recursively $2m + 1$ new sets of points, $\{\mathbf{r}_i^k\}_{i=0}^{2m+1-k}$, $k = 1, \dots, 2m + 1$, each having one fewer point than the previous one. At each level k , the new set of points is obtained as a convex combination of two consecutive points in the previous level. Instead of computing smaller and smaller sets of control points, Woźny and Chudy's method consists in $2m + 1$ convex combinations, each of them adding the contribution of one of the initial control points. A graphical layout of the algorithm can be seen in the first row of [Figure 3](#).

The new algorithm proposed here fuses in a way both de Casteljaeu's and Woźny-Chudy's approaches. The idea is to first compute a new set of control vertices, $\{\mathbf{r}_i^1\}_{i=0}^{2m}$,

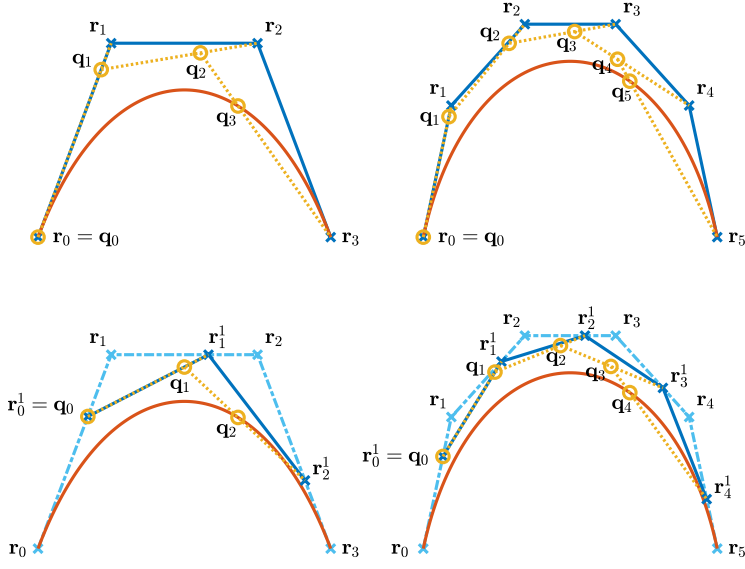


FIG. 3. Geometrical comparison between Wozny-Chudy's evaluation algorithm (first row) and the new proposed method (second row) when applied to a curve in \mathcal{EP}_1^ω (first column) and a curve in \mathcal{EP}_2^ω (second column).

starting from the initial control points, similar to a de Casteljau's step. These new vertices are computed such that the associated polynomial Bézier curve of degree $2m$ has the same evaluation as $\mathbf{r}(t)$ at the desired point $\hat{t} \in (0, 1)$, i.e., $\mathbf{r}(\hat{t}) = \sum_{i=0}^{2m} \mathbf{r}_i^1 B_{i,2m}(\hat{t})$, where the right-hand side can be efficiently computed via Wozny-Chudy's for polynomial curves, which is much faster than its specialized version for EPH curves. The detailed steps of the method are described in [Algorithm 6.3](#), where, for $m = 1$,

$$\begin{aligned} \tau_{0,1}^\omega(t) &= \frac{\sinh(\omega(t-1)) - \omega(t-1)}{(\omega - \sinh(\omega))(t-1)^2}, \\ \tau_{1,1}^\omega(t) &= \frac{\frac{\omega}{2} - \sinh(\omega) + \frac{\omega \cosh(\omega)}{2}}{\omega - 2 \sinh(\omega) + \omega \cosh(\omega)} - \frac{\frac{\sinh(\omega(t-1))}{2} + \frac{\sinh(t\omega)}{2} + \frac{\sinh(\omega)}{2} - t \sinh(\omega)}{t(t-1)(\omega - 2 \sinh(\omega) + \omega \cosh(\omega))}, \\ \tau_{2,1}^\omega(t) &= \frac{\sinh(t\omega) - t\omega}{t^2(\omega - \sinh(\omega))} + 1. \end{aligned}$$

and, for $m = 2$,

$$\begin{aligned} \tau_{0,2}^\omega(t) &= \frac{6\omega + 8 \sinh(\omega(t-1)) - \sinh(2\omega(t-1)) - 6t\omega}{(t-1)^4(6\omega + \sinh(2\omega) - 8 \sinh(\omega))}, \\ \tau_{1,2}^\omega(t) &= \frac{t-1}{4t} - \frac{3 \sinh(\frac{\omega}{2}) - 6 \sinh(\frac{\omega(2t-1)}{2}) - 2 \sinh(\frac{\omega(2t-3)}{2}) + \sinh(\frac{\omega(4t-3)}{2}) - 6\omega \cosh(\frac{\omega}{2}) + 6t\omega \cosh(\frac{\omega}{2})}{4t(t-1)^3(9 \sinh(\frac{\omega}{2}) + \sinh(\frac{3\omega}{2}) - 6\omega \cosh(\frac{\omega}{2}))}, \\ \tau_{2,2}^\omega(t) &= \frac{(3t+1)(t-1)}{6t^2} - \frac{\sinh(\omega(2t-1)) - 4 \sinh(\omega(t-1)) - 4 \sinh(t\omega) + 3 \sinh(\omega) + 2\omega(\cosh(\omega) + 2)(t-1)}{6t^2(t-1)^2(4\omega - 6 \sinh(\omega) + 2\omega \cosh(\omega))}, \\ \tau_{3,2}^\omega(t) &= \frac{3 \sinh(\frac{\omega}{2}) + 6 \sinh(\frac{\omega(2t-1)}{2}) + 2 \sinh(\frac{\omega(2t+1)}{2}) - \sinh(\frac{\omega(4t-1)}{2}) - 6t\omega \cosh(\frac{\omega}{2}) - t^4}{9 \sinh(\frac{\omega}{2}) + \sinh(\frac{3\omega}{2}) - 6\omega \cosh(\frac{\omega}{2})} + 1, \\ \tau_{4,2}^\omega(t) &= 1 - \frac{2 \sinh(t\omega)(\cosh(t\omega) - 4) + 6t\omega}{t^4(6\omega + 2 \sinh(\omega)(\cosh(\omega) - 4))}. \end{aligned}$$

As for the basis functions, the stable expressions for $\tau_{j,m}^\omega$ exploited in our implemen-

tation can be found in [Appendix K](#). A graphical layout of the algorithm can be seen in the second row of [Figure 3](#).

Algorithm 6.3 New proposal

```

Acquire  $\mathbf{r}_0, \dots, \mathbf{r}_{2m+1}, \hat{t}$ 
for  $j = 0, \dots, 2m$  do
   $\mathbf{r}_j^1 \leftarrow \tau_{j,m}^\omega(\hat{t})\mathbf{r}_j + (1 - \tau_{j,m}^\omega(\hat{t}))\mathbf{r}_{j+1}$ 
end for
 $\mathbf{q}_0 \leftarrow \mathbf{r}_0^1, h_0 \leftarrow 1$  and  $D \leftarrow \frac{1-\hat{t}}{\hat{t}}$ 
for  $k = 1, \dots, 2m$  do
   $h_k \leftarrow \left(1 + \frac{kD}{(2m+1-k)h_{k-1}}\right)^{-1}$  and  $\mathbf{q}_k \leftarrow (1 - h_k)\mathbf{q}_{k-1} + h_k\mathbf{r}_k^1$ 
end for
return  $\mathbf{q}_{2m}$ 

```

6.1. Comparing the three evaluation methods. We start comparing the behaviour of the three methods as ω goes to 0. In order to do so, we computed, for 500 equispaced values of $\omega \in (0, 2]$, the maximum over 100 curves with random control points uniformly distributed in $(0, 1)^d$ of the relative error in the infinity norm committed by each method in approximating the 5th order Taylor expansion of the curve at $\omega = 0$. In other words, in [Figure 4](#), one can see, for $d = 3$ and $m \in \{1, 2\}$, the behaviour of the function

$$(6.1) \quad \rho_{d,m}(\omega) := \max_{\{\mathbf{r}_i\}_{i=0}^{2m+1} \in \mathcal{R}} \frac{\left\| \sum_{i=0}^{2m+1} \mathbf{r}_i T_{i,m}^\omega(t) \Big|_{\mathbf{z}} - \sum_{i=0}^{2m+1} \mathbf{r}_i \phi_{i,m}^\omega(t) \Big|_{\mathbf{z}} \right\|_{\infty}}{\left\| \sum_{i=0}^{2m+1} \mathbf{r}_i T_{i,m}^\omega(t) \Big|_{\mathbf{z}} \right\|_{\infty}},$$

where \mathcal{R} is a collection of 100 random sets of $2m + 2$ control points in $(0, 1)^d$, $\mathbf{z} = [k/500]_{k=0}^{500}$ and $\sum_{i=0}^{2m+1} \mathbf{r}_i \phi_{i,m}^\omega(t) \Big|_{\mathbf{z}}$ is computed with each of the three considered methods. From a theoretical point of view, as ω gets closer and closer to 0, an exact evaluation of the curve should approach the evaluation of the polynomial curve obtained substituting each basis function $\phi_{i,m}^\omega$ with its corresponding Taylor polynomial, and thus we should get $\rho_{d,m}(\omega) \rightarrow 0$ for $\omega \rightarrow 0$. Since stability for small ω is not achievable, we have that, for each method, the value of $\rho_{d,m}(\omega)$ decreases until a certain threshold is met, under which $\rho_{d,m}(\omega)$ starts to increase and the method becomes unreliable. In particular, from [Figure 4](#) it is possible to see how the newly proposed algorithm is the one that can get the closest to 0 without having numerical issues. For the sake of completeness the points of minimum found for each graph are reported in [Table 2](#).

TABLE 2

Estimated $\bar{\omega} = \operatorname{argmin}_{\omega \in (0,2]} \rho_{d,m}(\omega)$ for $\rho_{d,m}(\omega)$ in (6.1) with $d = 3$ and $m \in \{1, 2\}$ for the three considered methods.

m	de Casteljau-like	Woźny-Chudy	New proposal
1	0.2760	0.2200	0.0960
2	1.1160	0.3800	0.1840

Concerning the running time of the three algorithms, fixed $d = 3$ and $m \in \{1, 2\}$, for each $\omega \in \{0.0960 + 2^k\}_{k=-50}^{50}$ we evaluated 10000 random curves at 501

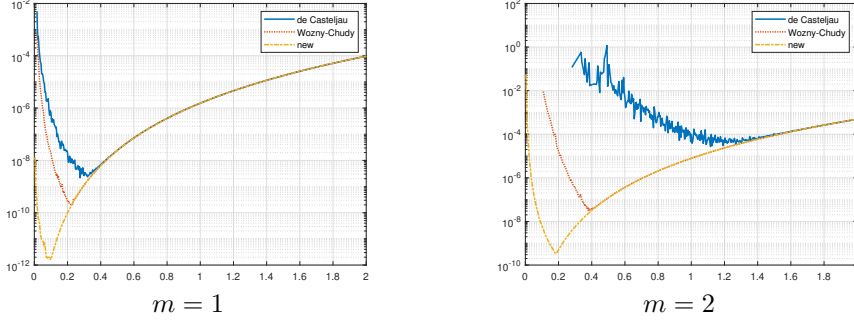


FIG. 4. The function $\rho_{d,m}(\omega)$ in (6.1) for $d = 3$ and $m \in \{1, 2\}$ computed with three different methods: the de Casteljaou-like B-algorithm, Woźny-Chudy's algorithm and the new proposed method.

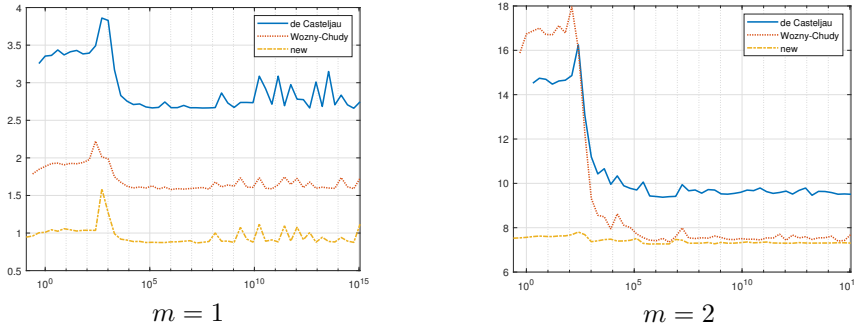


FIG. 5. Running times in seconds of the three considered methods for the evaluation of 10000 random curves, varying ω in $\{0.0920 + 2^k\}_{k=-50}^{50}$, for $d = 3$ and $m \in \{1, 2\}$.

equispaced points in $[0, 1]$. The results are visible in [Figure 5](#), where again the new proposed algorithm is the best performing one in both scenarios and for every value of ω considered. We observe that the slope around $\omega = 10^3$ is due to the fact that most of the exponential functions involved in the computations become very small and thus are set to 0, speeding up most computations. All numerical experiments were done in MATLAB 2021a on a laptop equipped with an Intel Core i7-10870H CPU and 32 GB RAM.

6.2. A note on a fourth algorithm. We conclude this section with a short discussion about the dynamic evaluation algorithm presented in [\[14, 15\]](#) which, although can be specialized for EPH curves, presents stability issues for large values of ω . To explain why this is the case, we begin with a brief review of the method. First, it must be that $\det([\mathbf{r}_{2m-d+2}, \dots, \mathbf{r}_{2m+1}]) \neq 0$. Then the method evaluates $\mathbf{r}(t)$ in $k \in \mathbb{N} \setminus \{1\}$ equispaced points over $[0, 1]$, finding $\mathbf{y}_i = \mathbf{r}(ih) \in \mathbb{R}^d$, where $h = 1/(k-1)$. Once the matrices $\mathbf{R}_1 := [\mathbf{r}_0, \dots, \mathbf{r}_{2m-d+1}] \in \mathbb{R}^{d \times (2m-d+2)}$ and $\mathbf{R}_2 := [\mathbf{r}_{2m-d+2}, \dots, \mathbf{r}_{2m+1}] \in \mathbb{R}^{d \times d}$ are defined, the problem is lifted to dimension $2m+2$, where the new control points are the columns of $\mathbf{R} := \begin{bmatrix} \mathbf{R}_1 & \mathbf{R}_2 \\ \mathbf{I}_{2m-d+2} & \mathbf{O}_{(2m-d+2) \times d} \end{bmatrix} \in \mathbb{R}^{(2m+2) \times (2m+2)}$, where \mathbf{I}_{2m-d+2} is the $(2m-d+2)$ -dimensional identity matrix and $\mathbf{O}_{(2m-d+2) \times d}$ is a $(2m-d+2) \times d$ matrix of zeros. It is easy to see that \mathbf{R} is invertible with $\mathbf{R}^{-1} = \begin{bmatrix} \mathbf{O}_{(2m-d+2) \times d} & \mathbf{I}_{2m-d+2} \\ \mathbf{R}_2^{-1} & \mathbf{R}_2^{-1} \mathbf{R}_1 \end{bmatrix}$. Now consider the following recursion:

$$(6.2) \quad \mathbf{z}_0 = \mathbf{R} \mathbf{e}_1, \quad \mathbf{z}_i = \mathbf{M} \mathbf{z}_{i-1} = \mathbf{M}^i \mathbf{z}_0, \quad i = 1, \dots, k-1,$$

where $\mathbf{e}_1 = [\delta_{1,j}]_{j=1}^{2m+2}$, $\delta_{i,j}$ being the Kronecker delta, $\mathbf{M} = \mathbf{R}\mathbf{C}_{h,m}^\omega \mathbf{R}^{-1}$, and $\mathbf{C}_{h,m}^\omega \in \mathbb{R}^{(2m+2) \times (2m+2)}$ is the unique matrix such that

$$\begin{bmatrix} \phi_{0,m}^\omega(t+h) \\ \vdots \\ \phi_{2m+1,m}^\omega(t+h) \end{bmatrix} = \mathbf{C}_{h,m}^\omega \begin{bmatrix} \phi_{0,m}^\omega(t) \\ \vdots \\ \phi_{2m+1,m}^\omega(t) \end{bmatrix}, \quad 0 \leq t+h \leq 1, t \in [0,1].$$

Then $\mathbf{y}_i = [\mathbf{I}_d, \mathbf{O}_{d \times (2m+2)}] \mathbf{z}_i$, $i = 0, \dots, k-1$. In other words, once we have the evaluations of the lifted curve $\{\mathbf{z}_i\}_{i=0}^{k-1}$, we only need to consider the first d components to find the solution for the initial low-dimensional problem.

Let us now focus on the space \mathcal{EP}_1^ω . To use the previous method we need to compute the matrix $\mathbf{C}_{h,1}^\omega$. Since

$$\begin{bmatrix} \phi_{0,1}^\omega(t) \\ \phi_{1,1}^\omega(t) \\ \phi_{2,1}^\omega(t) \\ \phi_{3,1}^\omega(t) \end{bmatrix} = \mathbf{B} \begin{bmatrix} 1 \\ t \\ e^{\omega t} \\ e^{-\omega t} \end{bmatrix}, \quad \text{with} \quad \mathbf{B} = \begin{bmatrix} 1 & 1 & 1 & 1 \\ 0 & c_2(\omega) & 1 - c_2(\omega) & 1 \\ 1 & 1 & -1 - \omega^2 c_1(\omega) & \cosh(\omega) \\ 0 & \omega c_2(\omega) & \omega(1 - c_2(\omega)) & \sinh(\omega) \end{bmatrix}$$

and

$$\begin{bmatrix} 1 \\ t \\ e^{\omega(t+h)} \\ e^{-\omega(t+h)} \end{bmatrix} = \widehat{\mathbf{C}}_{h,1}^\omega \begin{bmatrix} 1 \\ t \\ e^{\omega t} \\ e^{-\omega t} \end{bmatrix}, \quad \text{with} \quad \widehat{\mathbf{C}}_{h,1}^\omega = \begin{bmatrix} 1 & 0 & 0 & 0 \\ h & 1 & 0 & 0 \\ 0 & 0 & e^{\omega h} & 0 \\ 0 & 0 & 0 & e^{-\omega h} \end{bmatrix},$$

we have that

$$\begin{bmatrix} \phi_{0,1}^\omega(t+h) \\ \phi_{1,1}^\omega(t+h) \\ \phi_{2,1}^\omega(t+h) \\ \phi_{3,1}^\omega(t+h) \end{bmatrix} = \mathbf{C}_{h,1}^\omega \begin{bmatrix} \phi_{0,1}^\omega(t) \\ \phi_{1,1}^\omega(t) \\ \phi_{2,1}^\omega(t) \\ \phi_{3,1}^\omega(t) \end{bmatrix}, \quad \text{with} \quad \mathbf{C}_{h,1}^\omega = \mathbf{B} \widehat{\mathbf{C}}_{h,1}^\omega \mathbf{B}^{-1}.$$

In particular, it can be shown that

$$\begin{aligned} \mathbf{C}_{h,1}^\omega(4,4) &= \frac{\sinh(\omega(1+h)) - \omega(1+h)}{\sinh(\omega) - \omega} = \frac{e^{\omega(1+h)} - e^{-\omega(1+h)} - 2\omega(1+h)}{e^\omega - e^{-\omega} - 2\omega} \\ &= e^{\omega h} \frac{1 - e^{-2\omega(1+h)} - 2\omega e^{-\omega(1+h)}}{1 - e^{-2\omega} - 2\omega e^{-\omega}} = \mathcal{O}(e^{\omega h}) \quad \text{for} \quad \omega \rightarrow +\infty, \end{aligned}$$

since $h \in (0,1]$. This fact propagates to \mathbf{M} and its powers during the recursion (6.2) which ends with \mathbf{M}^{k-1} having an element that is $\mathcal{O}(e^\omega)$, making the computations numerically unstable already for ω of order 10^1 . In a similar way it is possible to check that the same happens for the space \mathcal{EP}_2^ω . Thus, it is not advisable to use this evaluation method in the context here described.

Appendix A. Proof of Proposition 3.2.

Proof. (a) is a consequence of the fact that $\phi_{i,1}^\omega(t) \geq 0$ for all $t \in [0,1]$ and $\sum_{i=0}^3 \phi_{i,1}^\omega(t) = 1$ for all $t \in [0,1]$;
 (b) is due to the fact that $\phi_{i,1}^\omega(t) = \phi_{3-i,1}^\omega(1-t)$ for all $t \in [0,1]$, $i = 0, \dots, 3$;

(c) follows from the fact that

$$\begin{aligned}\frac{d}{dt}\phi_{0,1}^\omega(t) &= -\delta_{0,1}^\omega \varphi_{0,1}^\omega(t), \\ \frac{d}{dt}\phi_{i,1}^\omega(t) &= \delta_{i-1,1}^\omega \varphi_{i-1,1}^\omega(t) - \delta_{i,1}^\omega \varphi_{i,1}^\omega(t), \quad i = 1, 2 \\ \frac{d}{dt}\phi_{3,1}^\omega(t) &= \delta_{2,1}^\omega \varphi_{2,1}^\omega(t);\end{aligned}$$

(d) is a consequence of (c).

Appendix B. Proof of Proposition 3.3.

Proof. By substituting (3.9) into (2.5) we obtain

$$\mathbf{r}'(t) = \mathbf{A}_0 \mathbf{i} \mathbf{A}_0^* \psi_{0,1}^\omega(t)^2 + (\mathbf{A}_0 \mathbf{i} \mathbf{A}_1^* + \mathbf{A}_1 \mathbf{i} \mathbf{A}_0^*) \psi_{0,1}^\omega(t) \psi_{1,1}^\omega(t) + \mathbf{A}_1 \mathbf{i} \mathbf{A}_1^* \psi_{1,1}^\omega(t)^2$$

and thus, in light of (3.3),

$$(B.1) \quad \mathbf{r}'(t) = \mathbf{A}_0 \mathbf{i} \mathbf{A}_0^* \varphi_{0,1}^\omega(t) + (\mathbf{A}_0 \mathbf{i} \mathbf{A}_1^* + \mathbf{A}_1 \mathbf{i} \mathbf{A}_0^*) \frac{1}{2} c_0(\omega) \varphi_{1,1}^\omega(t) + \mathbf{A}_1 \mathbf{i} \mathbf{A}_1^* \varphi_{2,1}^\omega(t).$$

Since $\mathbf{r}(t) = \mathbf{r}_0 + \int_0^t \mathbf{r}'(x) dx$, by integrating the expression in (B.1) exploiting the formulae in (3.5) and (3.8), we obtain the Bézier-like form of $\mathbf{r}(t)$ with control points in (3.11). \square

Appendix C. Proof of Proposition 3.5.

Proof. Since $\sigma(t) = \mathbf{A}(t) \mathbf{A}^*(t)$, in light of (3.9) we can write

$$\sigma(t) = |\mathbf{A}_0|^2 \psi_{0,1}^\omega(t)^2 + (\mathbf{A}_1 \mathbf{A}_0^* + \mathbf{A}_0 \mathbf{A}_1^*) \psi_{0,1}^\omega(t) \psi_{1,1}^\omega(t) + |\mathbf{A}_1|^2 \psi_{1,1}^\omega(t)^2.$$

Then, exploiting (3.3), the claimed result is obtained. \square

Appendix D. Proof of Proposition 3.6.

Proof. Since

$$s(t) = \int_0^t \sigma(x) dx = \int_0^t \sum_{i=0}^2 \sigma_i \varphi_{i,1}^\omega(x) dx = \sum_{i=0}^2 \sigma_i \int_0^t \varphi_{i,1}^\omega(x) dx,$$

then, recalling formulae (3.5) we arrive at

$$\begin{aligned}s(t) &= \sigma_2 c_2(\omega) \phi_{3,1}^\omega(t) \\ &+ \sigma_1 \left(-c_1(\omega) (\phi_{0,1}^\omega(t) + \phi_{1,1}^\omega(t)) + \left(-c_1(\omega) + \frac{c_3(\omega)}{c_0(\omega)} \right) (\phi_{2,1}^\omega(t) + \phi_{3,1}^\omega(t)) \right) \\ &+ \sigma_0 \left(c_1(\omega) \phi_{0,1}^\omega(t) + (c_1(\omega) + c_2(\omega)) (\phi_{1,1}^\omega(t) + \phi_{2,1}^\omega(t) + \phi_{3,1}^\omega(t)) \right)\end{aligned}$$

and, by collecting the coefficients of each basis function $\phi_{i,1}^\omega(t)$, $i = 0, \dots, 3$, we get the claimed result. \square

Appendix E. Proof of Proposition 4.2.

Proof. (a) is a consequence of the fact that $\phi_{i,2}^\omega(t) \geq 0$ for all $t \in [0, 1]$ and $\sum_{i=0}^5 \phi_{i,2}^\omega(t) = 1$ for all $t \in [0, 1]$;

(b) is due to the fact that $\phi_{i,2}^\omega(t) = \phi_{5-i,2}^\omega(1-t)$ for all $t \in [0, 1]$, $i = 0, \dots, 5$;
(c) follows from the fact that

$$\begin{aligned}\frac{d}{dt}\phi_{0,2}^\omega(t) &= -\epsilon_{0,2}^\omega \varphi_{0,2}^\omega(t), \\ \frac{d}{dt}\phi_{i,2}^\omega(t) &= \epsilon_{i-1,2}^\omega \varphi_{i-1,2}^\omega(t) - \epsilon_{i,2}^\omega \varphi_{i,2}^\omega(t), \quad i = 1, \dots, 4 \\ \frac{d}{dt}\phi_{5,2}^\omega(t) &= \epsilon_{4,2}^\omega \varphi_{4,2}^\omega(t);\end{aligned}$$

(d) is a consequence of (c). \square

Appendix F. Proof of Proposition 4.3.

Proof. By substituting (4.8) into (2.5) we obtain

$$\begin{aligned}\mathbf{r}'(t) &= \sum_{j=0}^2 \mathbf{A}_j \mathbf{iA}_j^* \psi_{j,2}^\omega(t)^2 + (\mathbf{A}_0 \mathbf{iA}_1^* + \mathbf{A}_1 \mathbf{iA}_0^*) \psi_{0,2}^\omega(t) \psi_{1,2}^\omega(t) \\ &\quad + (\mathbf{A}_1 \mathbf{iA}_2^* + \mathbf{A}_2 \mathbf{iA}_1^*) \psi_{1,2}^\omega(t) \psi_{2,2}^\omega(t) + (\mathbf{A}_0 \mathbf{iA}_2^* + \mathbf{A}_2 \mathbf{iA}_0^*) \psi_{0,2}^\omega(t) \psi_{2,2}^\omega(t)\end{aligned}$$

and thus, in light of (4.1) and (4.7),

$$\begin{aligned}\text{(F.1)} \quad \mathbf{r}'(t) &= \mathbf{A}_0 \mathbf{iA}_0^* \varphi_{0,2}^\omega(t) + (\mathbf{A}_0 \mathbf{iA}_1^* + \mathbf{A}_1 \mathbf{iA}_0^*) \frac{1}{2} \varphi_{1,2}^\omega(t) \\ &\quad + \left(\mathbf{A}_1 \mathbf{iA}_1^* q_0(\omega) + (\mathbf{A}_0 \mathbf{iA}_2^* + \mathbf{A}_2 \mathbf{iA}_0^*) \frac{1}{2} q_1(\omega) \right) \varphi_{2,2}^\omega(t) \\ &\quad + (\mathbf{A}_1 \mathbf{iA}_2^* + \mathbf{A}_2 \mathbf{iA}_1^*) \frac{1}{2} \varphi_{3,2}^\omega(t) + \mathbf{A}_2 \mathbf{iA}_2^* \varphi_{4,2}^\omega(t).\end{aligned}$$

Since $\mathbf{r}(t) = \mathbf{r}_0 + \int_0^t \mathbf{r}'(x) dx$, by integrating the expression in (F.1) exploiting the formulae in (4.3) and (4.7), we obtain the Bézier-like form of $\mathbf{r}(t)$ with control points in (4.10). \square

Appendix G. Proof of Proposition 4.5.

Proof. Since $\sigma(t) = \mathbf{A}(t)\mathbf{A}^*(t)$, in light of (4.8) we can write

$$\begin{aligned}\sigma(t) &= \sum_{j=0}^2 |\mathbf{A}_j|^2 \psi_{j,2}^\omega(t)^2 + (\mathbf{A}_1 \mathbf{A}_0^* + \mathbf{A}_0 \mathbf{A}_1^*) \psi_{0,2}^\omega(t) \psi_{1,2}^\omega(t) \\ &\quad + (\mathbf{A}_1 \mathbf{A}_2^* + \mathbf{A}_2 \mathbf{A}_1^*) \psi_{1,2}^\omega(t) \psi_{2,2}^\omega(t) + (\mathbf{A}_2 \mathbf{A}_0^* + \mathbf{A}_0 \mathbf{A}_2^*) \psi_{0,2}^\omega(t) \psi_{2,2}^\omega(t).\end{aligned}$$

Then, exploiting (4.1) and (4.7) we obtain the claimed result. \square

Appendix H. Proof of Proposition 4.6.

Proof. Since

$$s(t) = \int_0^t \sigma(x) dx = \int_0^t \sum_{i=0}^4 \sigma_i \varphi_{i,2}^\omega(x) dx = \sum_{i=0}^4 \sigma_i \int_0^t \varphi_{i,2}^\omega(x) dx,$$

recalling formulae (4.3), we then arrive at

$$\begin{aligned}
s(t) &= \sigma_0 \left(p_0(\omega) \phi_{0,2}^\omega(t) + (p_0(\omega) + q_2(\omega)) \sum_{i=1}^5 \phi_{i,2}^\omega(t) \right) \\
&\quad + \sigma_1 \left(p_1(\omega) (\phi_{0,2}^\omega(t) + \phi_{1,2}^\omega(t)) + (p_1(\omega) + q_3(\omega)) \sum_{i=2}^5 \phi_{i,2}^\omega(t) \right) \\
&\quad + \sigma_2 \left(p_2(\omega) \sum_{i=0}^2 \phi_{i,2}^\omega(t) + \left(p_2(\omega) + \frac{q_4(\omega)}{q_1(\omega)} \right) \sum_{i=3}^5 \phi_{i,2}^\omega(t) \right) \\
&\quad + \sigma_3 \left(p_3(\omega) \sum_{i=0}^3 \phi_{i,2}^\omega(t) + (p_3(\omega) + q_3(\omega)) (\phi_{4,2}^\omega(t) + \phi_{5,2}^\omega(t)) \right) + \sigma_4 q_2(\omega) \phi_{5,2}^\omega(t).
\end{aligned}$$

By collecting the coefficients of each basis function $\phi_{i,2}^\omega(t)$, $i = 0, \dots, 5$, we get the claimed result. \square

Appendix I. 5th order Taylor expansions at $\omega = 0$ of $\{\phi_{j,m}^\omega(t)\}_{j=0}^{2m+1}$, $m \in \{1, 2\}$. For $\{\phi_{j,1}^\omega(t)\}_{j=0}^3$,

$$\begin{aligned}
T_{0,1}^\omega(t) &= T_{3,1}^\omega(1-t), & T_{1,1}^\omega(t) &= T_{2,1}^\omega(1-t), \\
T_{2,1}^\omega(t) &= 3t^2(1-t) \frac{(30t^4 - 40t^3 + 23t^2 - 12t - 3)\omega^4 + 420(3t^2 - 2t + 1)\omega^2 + 25200}{25200}, \\
T_{3,1}^\omega(t) &= t^3 \frac{(10t^4 - 21t^2 + 11)\omega^4 + 420(t^2 - 1)\omega^2 + 8400}{8400},
\end{aligned}$$

and, for $\{\phi_{j,2}^\omega(t)\}_{j=0}^5$,

$$\begin{aligned}
T_{0,2}^\omega(t) &= T_{5,2}^\omega(1-t), & T_{1,2}^\omega(t) &= T_{4,2}^\omega(1-t), & T_{2,2}^\omega(t) &= T_{3,2}^\omega(1-t), \\
T_{3,2}^\omega(t) &= 10t^3(1-t)^2 \frac{(245t^4 - 392t^3 + 253t^2 - 82t + 3)\omega^4 + 420(10t^2 - 8t + 3)\omega^2 + 35280}{35280}, \\
T_{4,2}^\omega(t) &= 5t^4(1-t) \frac{(245t^4 - 196t^3 - 96t^2 + 44t - 1)\omega^4 + 840(5t^2 - 2t - 1)\omega^2 + 35280}{35280}, \\
T_{5,2}^\omega(t) &= t^5 \frac{(49t^4 - 100t^2 + 51)\omega^4 + 840(t^2 - 1)\omega^2 + 7056}{7056}.
\end{aligned}$$

Appendix J. Stable expressions of $\{\phi_{j,m}^\omega(t)\}_{j=0}^{2m+1}$, $m \in \{1, 2\}$, for large ω .

For $m = 1$,

$$\begin{aligned}
\phi_{0,1}^\omega(t) &= \phi_{3,1}^\omega(1-t), & \phi_{1,1}^\omega(t) &= \phi_{2,1}^\omega(1-t), \\
\phi_{2,1}^\omega(t) &= \frac{N\phi_{2,1}^\omega(t)}{D\phi_{2,1}^\omega(t)}, & \phi_{3,1}^\omega(t) &= \frac{e^{-2\omega t} + 2\omega t e^{-\omega t} - 1}{e^{-2\omega} + 2\omega e^{-\omega} - 1} e^{\omega(t-1)},
\end{aligned}$$

where

$$\begin{aligned}
N\phi_{2,1}^\omega(t) &= \left(\frac{1}{\omega} + t\right) e^{-3\omega} - \frac{1}{\omega} e^{\omega(t-3)} - \left(\frac{1}{\omega} + 1\right) e^{-\omega(t+2)} - \left(\frac{1}{\omega} + 3t - 2\right) e^{-2\omega} \\
&\quad + \left(\frac{2}{\omega} - 1\right) e^{\omega(t-2)} + \left(\frac{2}{\omega} + 1\right) e^{-\omega(t+1)} \\
&\quad - \left(\frac{1}{\omega} - 3t + 2\right) e^{-\omega} - \left(\frac{1}{\omega} - 1\right) e^{\omega(t-1)} - \frac{1}{\omega} e^{-t\omega} + \frac{1}{\omega} - t, \\
D\phi_{2,1}^\omega &= \left(\frac{2}{\omega} + 1\right) e^{-3\omega} - \left(\frac{2}{\omega} - 5 - 2\omega\right) e^{-2\omega} - \left(\frac{2}{\omega} + 5 - 2\omega\right) e^{-\omega} + \frac{2}{\omega} - 1,
\end{aligned}$$

and, for $m = 2$,

$$\phi_{0,2}^\omega(t) = \phi_{5,2}^\omega(1-t), \quad \phi_{1,2}^\omega(t) = \phi_{4,2}^\omega(1-t), \quad \phi_{2,2}^\omega(t) = \phi_{3,2}^\omega(1-t),$$

$$\phi_{3,2}^\omega(t) = \frac{N\phi_{3,2}^\omega(t)}{D\phi_{3,2}^\omega}, \quad \phi_{4,2}^\omega(t) = \frac{N\phi_{4,2}^\omega(t)}{D\phi_{4,2}^\omega} e^{\omega(t-1)},$$

$$\phi_{5,2}^\omega(t) = \frac{e^{-4\omega t} - 8e^{-3\omega t} - 12\omega t e^{-2\omega t} + 8e^{-\omega t} - 1}{e^{-4\omega} - 8e^{-3\omega} - 12\omega e^{-2\omega} + 8e^{-\omega} - 1} e^{2\omega(t-1)},$$

where

$$\begin{aligned}
N\phi_{3,2}^\omega(t) &= \left(\frac{3}{\omega} + 2t\right) e^{-5\omega} - \frac{4}{\omega} e^{\omega(t-5)} + \frac{1}{\omega} e^{\omega(2t-5)} - 4\left(\frac{2}{\omega} + 1\right) e^{-\omega(t+4)} \\
&\quad + \left(\frac{9}{\omega} - 2(5t-6)\right) e^{-4\omega} - 4\left(\frac{1}{\omega} + 3\right) e^{\omega(t-4)} + \left(\frac{3}{\omega} + 4\right) e^{2\omega(t-2)} \\
&\quad + \left(\frac{5}{\omega} + 2\right) e^{-\omega(2t+3)} + 4\left(\frac{1}{\omega} - 1\right) e^{-\omega(t+3)} - 4\left(\frac{3}{\omega} - 5t\right) e^{-3\omega} \\
&\quad + 4\left(\frac{3}{\omega} + 1\right) e^{\omega(t-3)} - \left(\frac{9}{\omega} + 2\right) e^{\omega(2t-3)} - \left(\frac{9}{\omega} - 2\right) e^{-2\omega(t+1)} + 4\left(\frac{3}{\omega} - 1\right) e^{-\omega(t+2)} \\
&\quad - 4\left(\frac{3}{\omega} + 5t\right) e^{-2\omega} + 4\left(\frac{1}{\omega} + 1\right) e^{\omega(t-2)} + \left(\frac{5}{\omega} - 2\right) e^{2\omega(t-1)} \\
&\quad + \left(\frac{3}{\omega} - 4\right) e^{-\omega(2t+1)} - 4\left(\frac{1}{\omega} - 3\right) e^{-\omega(t+1)} + \left(\frac{9}{\omega} + 2(5t-6)\right) e^{-\omega} \\
&\quad - 4\left(\frac{2}{\omega} - 1\right) e^{\omega(t-1)} + \frac{1}{\omega} e^{-2\omega t} - \frac{4}{\omega} e^{-\omega t} + \frac{3}{\omega} - 2t,
\end{aligned}$$

$$D\phi_{3,2}^\omega = 2 \left[\left(\frac{3}{\omega} + 1 \right) e^{-5\omega} + \left(\frac{27}{\omega} + 31 + 6\omega \right) e^{-4\omega} - 2 \left(\frac{15}{\omega} - 23 - 15\omega \right) e^{-3\omega} \right. \\ \left. - 2 \left(\frac{15}{\omega} + 23 - 15\omega \right) e^{-2\omega} + \left(\frac{27}{\omega} - 31 + 6\omega \right) e^{-\omega} + \frac{3}{\omega} - 1 \right],$$

$$N\phi_{4,2}^\omega(t) = 2e^{-\omega(2t+5)} + 3(1+2\omega t)e^{-\omega(t+5)} - 6e^{-5\omega} + e^{\omega(t-5)} - 2e^{-\omega(3t+4)} \\ - 2e^{-2\omega(t+2)} - 3(9+10\omega t)e^{-\omega(t+4)} + 38e^{-4\omega} - 7e^{\omega(t-4)} \\ - (1+6\omega)e^{-3\omega(t+1)} + 24(1+\omega)e^{-\omega(2t+3)} + 12(2+\omega(5t-3))e^{-\omega(t+3)} \\ - 8(7-3\omega)e^{-3\omega} + 3(3-2\omega)e^{\omega(t-3)} + 3(3+2\omega)e^{-\omega(3t+2)} - 8(7+3\omega)e^{-2\omega(t+1)} \\ + 12(2-\omega(5t-3))e^{-\omega(t+2)} + 24(1-\omega)e^{-2\omega} - (1-6\omega)e^{\omega(t-2)} \\ - 7e^{-\omega(3t+1)} + 38e^{-\omega(2t+1)} - 3(9-10\omega t)e^{-\omega(t+1)} - 2e^{-\omega} \\ - 2e^{\omega(t-1)} + e^{-3\omega t} - 6e^{-2\omega t} + 3(1-2\omega t)e^{-\omega t} + 2,$$

$$D\phi_{4,2}^\omega = e^{-7\omega} + (1+6\omega)e^{-6\omega} - 27(3+2\omega)e^{-5\omega} + (79-156\omega-72\omega^2)e^{-4\omega} \\ + (79+156\omega-72\omega^2)e^{-3\omega} - 27(3-2\omega)e^{-2\omega} + (1-6\omega)e^{-\omega} + 1.$$

Appendix K. Stable expressions of $\{\tau_{j,m}^\omega(t)\}_{j=0}^{2m}$, $m \in \{1, 2\}$, for large ω .

For $m = 1$,

$$\tau_{0,1}^\omega(t) = \frac{e^{\omega(t-2)} - 2(t-1)\omega e^{-\omega} - e^{-t\omega}}{(t-1)^2(e^{-2\omega} + 2\omega e^{-\omega} - 1)}, \quad \tau_{1,1}^\omega(t) = \frac{N\tau_{1,1}^\omega(t)}{D\tau_{1,1}^\omega(t)}, \\ \tau_{2,1}^\omega(t) = \frac{t^2 e^{-2\omega} - e^{-\omega(t+1)} + 2t(t-1)\omega e^{-\omega} + e^{\omega(t-1)} - t^2}{t^2(e^{-2\omega} + 2\omega e^{-\omega} - 1)},$$

where

$$N\tau_{1,1}^\omega(t) = \left(\left(\frac{2}{\omega} + 1 \right) t^2 - \left(\frac{4}{\omega} + 1 \right) t + \frac{1}{\omega} \right) e^{-2\omega} - \frac{1}{\omega} e^{\omega(t-1)} \\ - \frac{1}{\omega} e^{\omega(t-2)} + 2t(t-1)e^{-\omega} + \frac{1}{\omega} e^{-t\omega} \\ + \frac{1}{\omega} e^{-\omega(t+1)} - \left(\frac{2}{\omega} - 1 \right) t^2 + \left(\frac{4}{\omega} - 1 \right) t - \frac{1}{\omega}, \\ D\tau_{1,1}^\omega(t) = 2t(t-1)(e^{-\omega} + 1) \left(\left(\frac{2}{\omega} + 1 \right) e^{-\omega} - \frac{2}{\omega} + 1 \right),$$

and, for $m = 2$, $\tau_{j,2}^\omega(t) = N\tau_{j,2}^\omega(t)/D\tau_{j,2}^\omega(t)$, $j = 0, \dots, 4$, where

$$N\tau_{0,2}^\omega(t) = -e^{2\omega(t-2)} + 8e^{\omega(t-3)} - 12(t-1)\omega e^{-2\omega} - 8e^{-\omega(t+1)} + e^{-2t\omega}, \\ D\tau_{0,2}^\omega(t) = (t-1)^4 (-e^{-4\omega} + 8e^{-3\omega} + 12\omega e^{-2\omega} - 8e^{-\omega} + 1),$$

$$\begin{aligned}
N\tau_{1,2}^\omega(t) &= (t-1)^4 e^{-3\omega} - 2e^{\omega(t-3)} + e^{\omega(2t-3)} \\
&\quad + 3(3t^4 - 12t^3 + 18t^2 - 12t + 2 + 2t\omega(t^3 - 4t^2 + 6t - 3)) e^{-2\omega} \\
&\quad\quad - 6e^{\omega(t-2)} + 6e^{-\omega(t+1)} \\
&\quad - 3(3t^4 - 12t^3 + 18t^2 - 12t + 2 - 2t\omega(t^3 - 4t^2 + 6t - 3)) e^{-\omega} \\
&\quad\quad - e^{-2t\omega} + 2e^{-t\omega} - (t-1)^4,
\end{aligned}$$

$$D\tau_{1,2}^\omega(t) = 4t(t-1)^3 (e^{-3\omega} + 3(2\omega+3)e^{-2\omega} + 3(2\omega-3)e^{-\omega} - 1),$$

$$\begin{aligned}
N\tau_{2,2}^\omega(t) &= - \left(\frac{3(6t^4 - 16t^3 + 12t^2 - 1)}{\omega} + 2t(3t^3 - 8t^2 + 6t - 1) \right) e^{-2\omega} \\
&\quad + \frac{4}{\omega} e^{\omega(t-2)} - \frac{1}{\omega} e^{2\omega(t-1)} - \frac{4}{\omega} e^{-\omega(t+1)} \\
&\quad + 8t(3t^3 - 8t^2 + 6t - 1) e^{-\omega} \\
&\quad + \frac{4}{\omega} e^{\omega(t-1)} + \frac{1}{\omega} e^{-2t\omega} - \frac{4}{\omega} e^{-t\omega} \\
&\quad - \frac{3(6t^4 - 16t^3 + 12t^2 - 1)}{\omega} + 2t(3t^3 - 8t^2 + 6t - 1),
\end{aligned}$$

$$D\tau_{2,2}^\omega(t) = 12t^2(t-1)^2 \left(\left(\frac{3}{\omega} + 1 \right) e^{-2\omega} + 4e^{-\omega} - \frac{3}{\omega} + 1 \right),$$

$$\begin{aligned}
N\tau_{3,2}^\omega(t) &= t^3(3t-4)e^{-3\omega} + 2e^{-\omega(t+2)} \\
&\quad + 3(2t\omega - 8t^3\omega + 6t^4\omega - 12t^3 + 9t^4 + 1) e^{-2\omega} \\
&\quad - 6e^{\omega(t-2)} + e^{2\omega(t-1)} - e^{-\omega(2t+1)} + 6e^{-\omega(t+1)} \\
&\quad + 3(2t\omega - 8t^3\omega + 6t^4\omega + 12t^3 - 9t^4 - 1) e^{-\omega} \\
&\quad\quad - 2e^{\omega(t-1)} - t^3(3t-4),
\end{aligned}$$

$$D\tau_{3,2}^\omega(t) = 4t^3(t-1)(e^{-3\omega} + 3(2\omega+3)e^{-2\omega} + 3(2\omega-3)e^{-\omega} - 1),$$

$$\begin{aligned}
N\tau_{4,2}^\omega(t) &= -t^4 e^{-4\omega} + 8t^4 e^{-3\omega} + e^{-2\omega(t+1)} - 8e^{-\omega(t+2)} \\
&\quad + 12t(t^3-1)\omega e^{-2\omega} + 8e^{\omega(t-2)} - e^{2\omega(t-1)} - 8t^4 e^{-\omega} + t^4,
\end{aligned}$$

$$D\tau_{4,2}^\omega(t) = t^4(-e^{-4\omega} + 8e^{-3\omega} + 12\omega e^{-2\omega} - 8e^{-\omega} + 1).$$

Acknowledgments. This work has been accomplished within the ‘‘Research Italian network on Approximation’’ (RITA) and the TAA-UMI group.

REFERENCES

- [1] J. M. CARNICER AND J. M. PEÑA, *Totally positive bases for shape preserving curve design and optimality of B-splines*, *Comput. Aided Geom. Design*, 11 (1994), pp. 633–654, [https://doi.org/10.1016/0167-8396\(94\)90056-6](https://doi.org/10.1016/0167-8396(94)90056-6).
- [2] I. CATTIAUX-HUILLARD AND L. SAINI, *Characterization and extensive study of cubic and quintic algebraic trigonometric planar PH curves*, *Adv. Comput. Math.*, 46 (2020), <https://doi.org/10.1007/s10444-020-09772-4>.
- [3] R. T. FAROUKI, *Pythagorean-hodograph curves: algebra and geometry inseparable*, vol. 1 of *Geometry and Computing*, Springer, Berlin, 2008, <https://doi.org/10.1007/978-3-540-73398-0>.
- [4] R. T. FAROUKI, M. AL KANDARI, AND T. SAKKALIS, *Hermite interpolation by rotation-invariant spatial Pythagorean-hodograph curves*, *Adv. Comput. Math.*, 17 (2002), pp. 369–383, <https://doi.org/10.1023/A:1016280811626>.
- [5] C. GONZÁLEZ, G. ALBRECHT, M. PALUSZNY, AND M. LENTINI, *Design of C^2 algebraic-trigonometric pythagorean hodograph splines with shape parameters*, *Comput. Appl. Math.*, 37 (2018), pp. 1472–1495, <https://doi.org/10.1007/s40314-016-0404-y>.
- [6] J. KOZAK, M. KRAJNC, M. ROGINA, AND V. VITRIH, *Pythagorean-hodograph cycloidal curves*, *J. Numer. Math.*, 23 (2015), pp. 345–360, <https://doi.org/10.1515/jnma-2015-0023>.
- [7] E. MAINAR AND J. M. PEÑA, *Corner cutting algorithms associated with optimal shape preserving representations*, *Comput. Aided Geom. Design*, 16 (1999), pp. 883–906, [https://doi.org/10.1016/S0167-8396\(99\)00035-7](https://doi.org/10.1016/S0167-8396(99)00035-7).
- [8] E. MAINAR AND J. M. PEÑA, *A general class of Bernstein-like bases*, *Comput. Math. Appl.*, 53 (2007), pp. 1686–1703, <https://doi.org/10.1016/j.camwa.2006.12.018>.
- [9] E. MAINAR AND J. M. PEÑA, *Optimal bases for a class of mixed spaces and their associated spline spaces*, *Comput. Math. Appl.*, 59 (2010), pp. 1509–1523, <https://doi.org/10.1016/j.camwa.2009.11.009>.
- [10] L. ROMANI AND F. MONTAGNER, *Algebraic-trigonometric Pythagorean-hodograph space curves*, *Adv. Comput. Math.*, 45 (2019), pp. 75–98, <https://doi.org/10.1007/s10444-018-9606-8>.
- [11] L. ROMANI, L. SAINI, AND G. ALBRECHT, *Algebraic-trigonometric Pythagorean-hodograph curves and their use for Hermite interpolation*, *Adv. Comput. Math.*, 40 (2014), pp. 977–1010, <https://doi.org/10.1007/s10444-013-9338-8>.
- [12] A. RÓTH, *Algorithm 992: an OpenGL- and C++-based function library for curve and surface modeling in a large class of extended Chebyshev spaces*, *ACM Trans. Math. Software*, 45 (2019), <https://doi.org/10.1145/3284979>.
- [13] P. WOŹNY AND F. CHUDY, *Linear-time geometric algorithm for evaluating Bézier curves*, *Comput.-Aided Des.*, 118 (2020), pp. 102760, 6, <https://doi.org/10.1016/j.cad.2019.102760>.
- [14] X. YANG AND J. HONG, *Dynamic evaluation of free-form curves and surfaces*, *SIAM J. Sci. Comput.*, 39 (2017), pp. B424–B441, <https://doi.org/10.1137/16M1058911>.
- [15] X. YANG AND J. HONG, *Dynamic evaluation of exponential polynomial curves and surfaces via basis transformation*, *SIAM J. Sci. Comput.*, 41 (2019), pp. A3401–A3420, <https://doi.org/10.1137/18M1230359>.